Results

ZNF216 directly binds to polyubiquitin

We have identified a gene, *Znf216* (*Za20d2*, Mouse Genome Informatics), encoding an A20 zinc-finger (Znf-A20) motif-containing protein, as a RANKL-induced gene upregulated upon osteoclast formation using a microarray technique (Hishiya *et al*, 2005). *Znf216* was originally identified as a candidate gene for hearing loss and is expressed in cochlear and skeletal muscle (Scott *et al*, 1998; Huang *et al*, 2004). To determine the function of ZNF216, we searched for molecules that associate with ZNF216 using yeast two-hybrid screening and isolated several clones encoding a gene for polyubiquitin C. To determine whether ZNF216 interacts with ubiquitin in mammalian cells, we transfected HEK293 cells with an expression vector for FLAG-tagged ZNF216 and HA-tagged ubiquitin and performed co-immunoprecipitation experiments. ZNF216 possesses A20-type (amino acids 11–35) and AN1-type (amino acids 154–191) zinc-finger domains at its N- and C-termini, respectively (Figure 1A). Endogenous ubiquitinylated proteins, which appear as smears, were co-immunoprecipitated with FLAG-tagged ZNF216 (Figure 1B). Notably, N-terminal deletion (ΔN; amino acids 36–213) or point mutants (M1 and M3) of the A20-type zinc-finger (ZnF-A20) domain abolished ubiquitin-binding ability of ZNF216, indicating that the ZnF-A20 domain is indispensable for binding to ubiquitin (Figures 1A and B). Whereas in non-denaturing conditions, ubiquitinylated molecules were present with FLAG-tagged ZNF216, these molecules completely disappear from immunoprecipitates following heat denaturation, which abolishes noncovalent protein–protein interactions (Figure 1C), suggesting that ZNF216 associates with ubiquitinylated proteins rather than being ubiquitinylated itself. Next, to determine whether ZNF216 binds to ubiquitin directly, we performed GST pull-down assays using GST-ZNF216 fusion proteins (Figure 1D) and purified polyubiquitin. As shown in Figure 1E, GST-ZNF216 but not GST bound to polyubiquitin chains. As expected, binding of ZNF216 to polyubiquitin chains was completely abolished by a point mutation in the ZnF-A20 domain (M1, Figure 1E). Furthermore, a GST fusion protein containing only the ZnF-A20 domain (amino acids 2–60) could bind to polyubiquitin chains, suggesting that ZNF216 directly binds to polyubiquitin chains, and that the ZnF-A20 domain is required for binding to polyubiquitin. As for other ZnF-A20 containing proteins, AWP1 (ZA20D3) also possessed polyubiquitin-binding activity but the ZnF-A20 domain(s) of Rabex-5 (Horiuchi *et al*, 1997) and A20/TNFAIP3 (Opipari *et al*, 1990) proteins did not (Supplementary Figure S1).

ZNF216 associates with the 26S proteasome

We also identified molecules associating with ZNF216 by proteomic analysis of complexes formed with FLAG-tagged ZNF216. Molecules expressed in HEK293 cells and that co-immunoprecipitated with FLAG-tagged ZNF216 were analyzed by tandem mass spectrometry. By this analysis, every subunit of the 26S proteasome complex was identified as associating with FLAG-tagged ZNF216 (data not shown). To identify the region of ZNF216 required for association with the 26S proteasome, lysates of cells expressing either FLAG-tagged ZNF216 or its mutants were immunoprecipitated with anti-FLAG antibody. Co-precipitation of proteasomal components was monitored by immunoblotting using an antibody against Rpn7p (S10a), a non-ATPase subunit of the 19S regulatory subunit. As shown in Figure 2A, this protein efficiently co-precipitated with FLAG-tagged ZNF216. The interaction was also observed with truncated or point mutants of ZnF-A20 (ΔN or M1), indicating that ubiquitin-binding ability is dispensable for association with the 26S proteasome. To determine whether endogenous ZNF216 proteins are also associated with the 26S proteasome, we performed a GST pull-down assay using the ubiquitin-like (Ubl) domain of hHR23B, a human homologue of Rad23, which is known to bind to the 26S proteasome. As shown in Figure 2B, GST-Ubl but not GST was pulled down with the endogenous 26S proteasome. Endogenous ZNF216 was also detected in the GST-Ubl/26S proteasome complex (upper panels, Figure 2B). Furthermore, purified recombinant ZNF216 did not bind to GST-Ubl (lower panel, Figure 2B), suggesting that endogenous ZNF216 is not directly bound to the Ubl domain but associates with the 26S proteasome.

Colocalization with the aggresome

Next, we determined the subcellular localization of ZNF216. Indirect immunofluorescence of ZNF216 expressed in COS-7 cells showed that the protein was largely cytoplasmic but was seen to a lesser extent in the nucleus (Figure 3A). Aggresomes, which are insoluble aggregates of ubiquitinylated proteins complexed with the proteasome and induced by treatment with proteasome inhibitors, are known to mimic inclusions seen in pathogenic UPS disorders (Johnston *et al*, 1998; Kopito, 2000; Lelouard *et al*, 2002). As shown in Figures 3D–H, ZNF216 proteins were colocalized with aggresomes induced by treatment with the proteasome inhibitor MG132. ZNF216 itself was not ubiquitinylated as shown in Figure 1C.

Induction of ZNF216 expression upon muscle atrophy

Biochemical and cell biological evidence presented here strongly suggests that ZNF216 functions in the UPS. In skeletal muscle, it is generally accepted that the UPS plays a critical role in muscular atrophy, and expression of atrophy-related genes including those encoding UPS components is induced in atrophying muscle (Jagoe *et al*, 2002; Lecker *et al*, 2004). As *Znf216* was predominantly expressed in brain and skeletal muscle (Scott *et al*, 1998), we investigated the relationship between ZNF216 and muscle atrophy. To determine whether *Znf216* expression is induced during muscle atrophy, an *in vitro* model of muscle atrophy was utilized. It has been reported that addition of dexamethasone to cultures of differentiated C2C12 myotubes causes formation of myotubes exhibiting signs of atrophy, including a reduction in myotube diameter (Stitt *et al*, 2004). Such treatment dramatically induced expression of *Znf216* (Figure 4A).

Next, expression of *Znf216* was determined in *in vivo* experimental models of muscle atrophy. Mice that undergo fasting for 2 days show significant decreases in body weight, as well as in the mass of the gastrocnemius muscles (data not shown). In this model, fasting for 2 days results in dramatic increases in *Znf216* mRNA (Figure 4B) and protein (Supplementary Figure S3) in muscle. Although there were differences in induction patterns of two differently sized transcripts of Znf216 by atrophy-inducting stimuli, both transcripts encode the same protein (Supplementary Figures

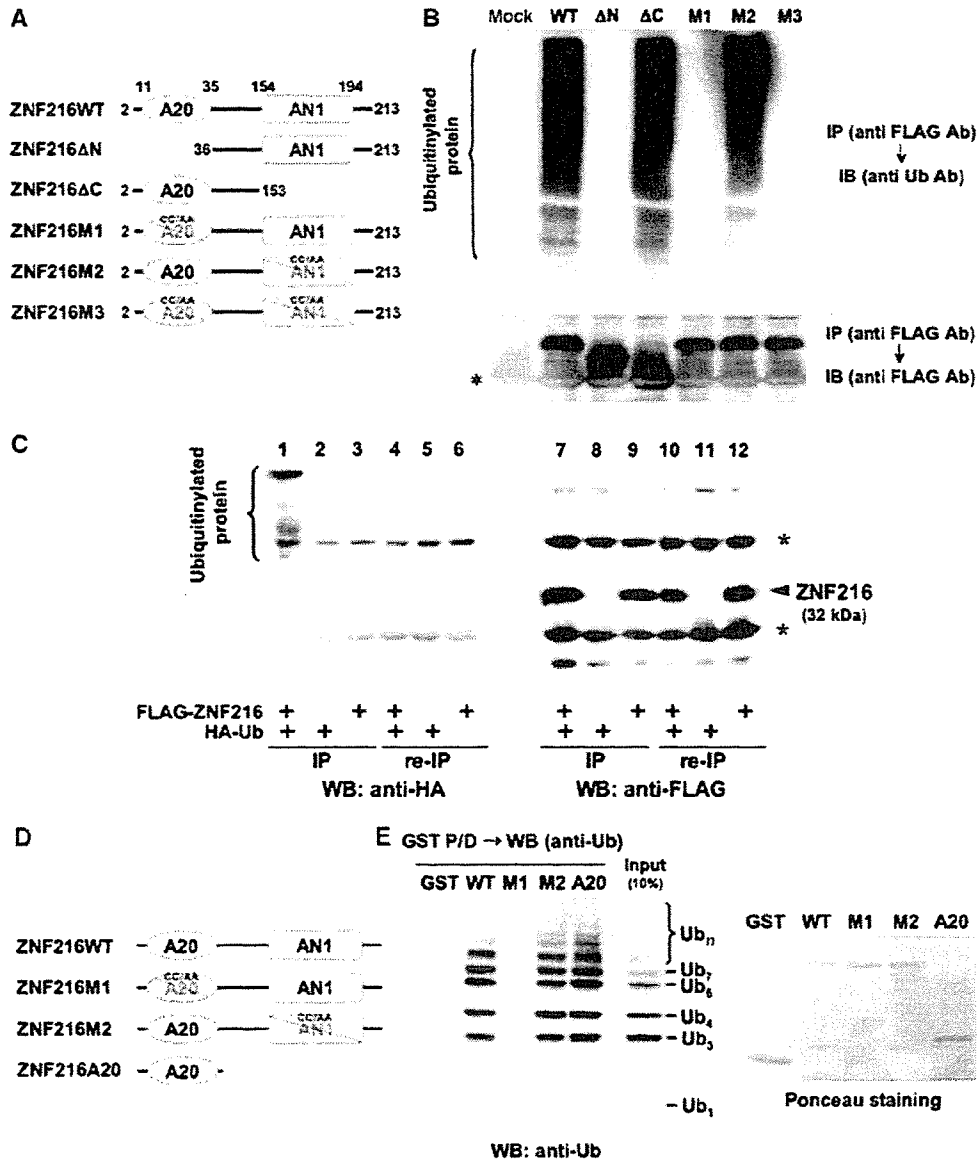

Figure 1 ZNF216 binds polyubiquitin directly through the ZnF-A20 domain. (**A**) Schematic representation of the primary structure of wild-type ZNF216 and its mutants. ZNF216ΔN (aa 36–213) and ZNF216ΔC (aa 2–153) constructs lack the ZnF-A20 (aa 11–35) and ZnF-AN1 (aa 154–194) domains, respectively. Cysteine residues at positions 30 and 33 within the ZnF-A20 were substituted with alanines (C30A/C33A) in ZNF216M1, and both cysteines 170 and 175 within the ZnF-AN1 were substituted with alanines (C170A/C175A) in ZNF216M2. Both ZnF-A20 and ZnF-AN1 domains were mutated in ZNF216M3. (**B**) Co-precipitation of ubiquitinylated proteins and ZNF216. FLAG-tagged ZNF216 or mutants were expressed in HEK293 cells, and cell extracts were immunoprecipitated with anti-FLAG antibody. Ubiquitinylated proteins detected with anti-ubiquitin antibody were precipitated with FLAG-tagged ZNF216 but not with ZnF-A20 mutants. Expression levels of FLAG-tagged ZNF216 constructs are shown at the bottom. Bands corresponding to immunoglobulin chains are marked by an asterisk. (**C**) ZNF216 is minimally ubiquitinylated. HEK293 cells expressing FLAG-tagged ZNF216 or HA-tagged ubiquitin were lysed and immunoprecipitation was performed using anti-FLAG antibody. Aliquots of precipitated beads were boiled and immunoprecipitated again (re-IP). Each sample was separated on gels and probed with anti-HA (left) or anti-FLAG antibody (right). Bands for immunoglobulin chains are marked by asterisks. (**D**) Constructs used for *in vitro* binding assay. ZNF216WT, ZNF216M1 and ZNF216 M2 were as indicated in (A). ZNF216A20 possesses only the A20 domain (aa 2–60). All constructs were produced as GST fusion proteins. (**E**) *In vitro* ubiquitin binding assay. Left panel: GST protein fused to the constructs indicated in (D) was incubated with purified K48-linked polyubiquitin chains, followed by precipitation with GSH beads. In all, 10% of purified polyubiquitin chains was separated without pull-down to evaluate protein amount (10% input). Right panel: the membrane was stained with ponceau to evaluate levels of GST fusion protein.

S2 and S3). Expression of MuRF-1 (Figure 4B) and MAFbx (Gomes *et al*, 2001) was also induced in fasting. Upregulation of *Znf216* was also observed in a model of denervation-induced muscle atrophy. Neurectomy promotes significant reduction (~20%) in the weight of gastrocnemius muscles within the first 7 days postsurgery. As expected, expression of *Znf216* and MuRF-1 was induced in gastrocnemius muscles by denervation-induced muscle atrophy (Figure 4C). These results suggest that *Znf216* expression is associated with atrophy in skeletal muscles.

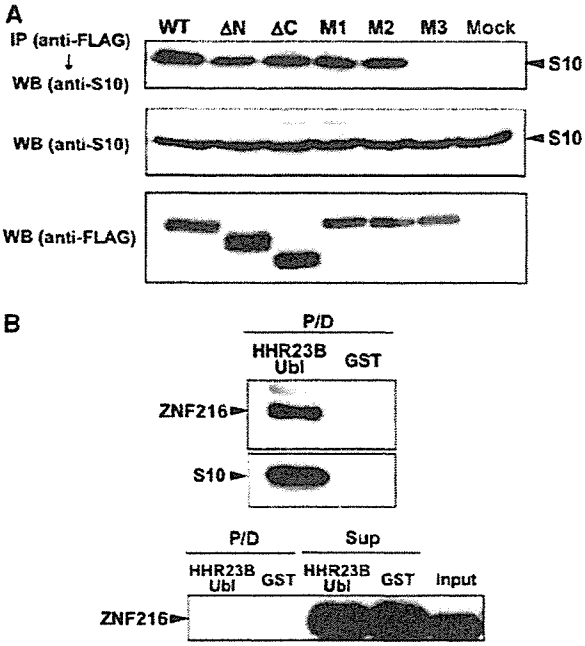

Figure 2 Interaction of ZNF216 with the 26S proteasome in mammalian cells. (**A**) Co-precipitation of the 26S proteasome and ZNF216. Co-precipitated proteins with FLAG-ZNF216 were resolved by SDS–PAGE and detected by immunoblotting using anti-S10a/Rpn7p antibody (anti-S10) or anti-FLAG antibody. Aliquots of cellular extracts were immunoblotted without immunoprecipitation to evaluate protein expression in the bottom panels. (**B**) ZNF216 was detected in the 26S proteasome fraction. Upper panel, cell lysates were incubated with a GST fusion of HHR23B Ubl (HHR23B Ubl) to isolate the 26S proteasome. Precipitated proteins (P/D) were separated and probed with anti-S10 or anti-ZNF216 antibody. Lower panel: purified recombinant ZNF216 was incubated with a GST fusion of HHR23B Ubl or GST protein. Precipitated (P/D) or not precipitated (Sup) proteins were probed with anti-ZNF216 antibody. No direct binding of ZNF216 to the Ubl domain of HHR23B was detected.

The transcription factor FOXO has been reported to play a critical role in muscular atrophy by inducing atrophy-related genes, including MAFbx/Atrogin-1 (Sandri *et al*, 2004; Stitt *et al*, 2004). Therefore, we asked whether FOXO activation upregulated *Znf216* expression. To do so, we employed a Cre-loxP system (Furukawa-Hibi *et al*, 2002) in which constitutively active FOXO4 (AFX-TM) created by mutation of the three Akt phosphorylation sites, T32A, S253A and S315A (Brunet *et al*, 1999), was expressed in C2C12-AFX-TM cells following infection by Cre recombinase-expressing adenovirus (Cre) (Figure 4D). Both AFX-TM mRNA and protein were induced 24 h after infection with Cre but not with control adenovirus (Furukawa-Hibi *et al*, 2002). ZNF216 mRNA was markedly increased in C2C12-AFX-TM cells as a result of infection with Cre but not following infection with control virus (Figure 4E). These results suggest that ZNF216 may function as a downstream effector of FOXO in muscle atrophy.

Generation of mice lacking ZNF216

To investigate the *in vivo* function of ZNF216, mice deficient for ZNF216 ($Znf216^{lex/lex}$) were generated by gene trapping at Omnibank of Lexicon Genetics (Zambrowicz *et al*, 1998). The structure of the predicted trapped gene is shown in Figure 5A. The trapping vector, VICTR48, was inserted 3.3 kbp upstream of exon 3, which encodes the first methionine of mouse *Znf216* (Figure 5A). $Znf216^{lex/lex}$ mice were born from interbred heterozygous $Znf216^{+/lex}$ mice in Mendelian ratios, indicating that ZNF216 is dispensable for embryogenesis or fetal development. No ZNF216 mRNA or protein was detected in $Znf216^{lex/lex}$ mice by Northern or immunoblot analyses, respectively (Figures 5B and C), indicating that the mice are ZNF216 nulls. Expression levels of ZNF216 in $Znf216^{+/lex}$ heterozygotes were nearly one-half those of wild-type mice. $Znf216^{lex/lex}$ mice were viable and fertile, without gross abnormalities or apparent pathological alteration, but they weighed less than sex- and age-matched controls (Figure 5D). At 45 weeks, the average weights of $Znf216^{+/+}$ and

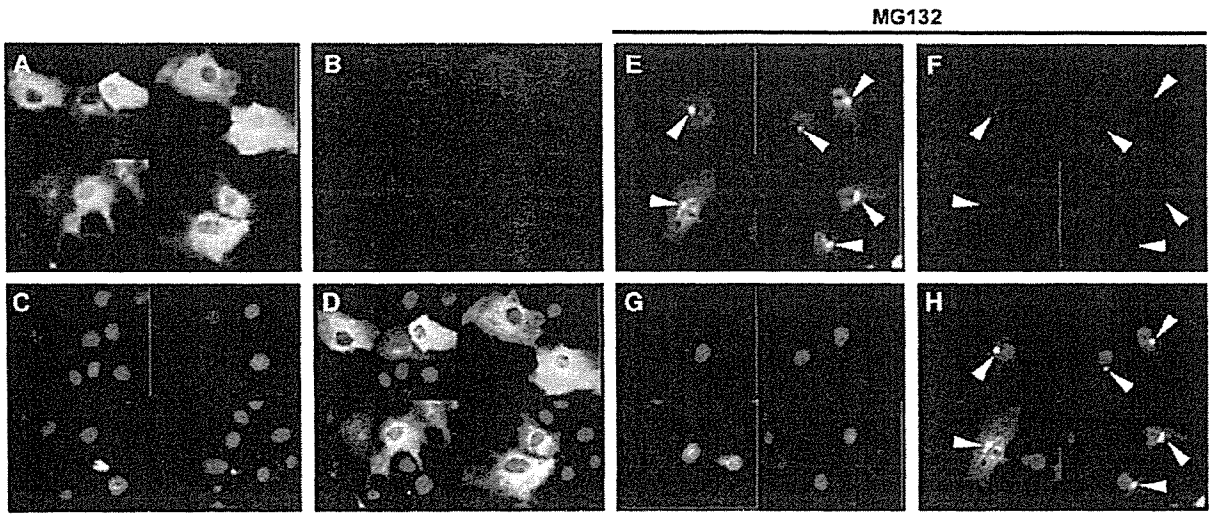

Figure 3 ZNF216 is localized in 'aggresomes' with ubiquitinylated proteins. (**A–H**) COS cells were transfected with expression vectors for FLAG-tagged ZNF216 and HA-tagged ubiquitin. Fixed cells were subjected to indirect immunofluorescence using (A, E) anti-FLAG (with AlexaFluor 488 anti-mouse IgG, green) and (B, F) anti-HA (with AlexaFluor 546 anti-rat IgG antibodies, red) antibodies. (C, G) Nuclei were stained with DAPI in the same fields of each panel. (E–H) Transfected COS cells were treated with the proteasome inhibitor, MG132 (0.5 μM). Aggresomes formed are indicated by arrowheads. The merged images were shown in (D and H).

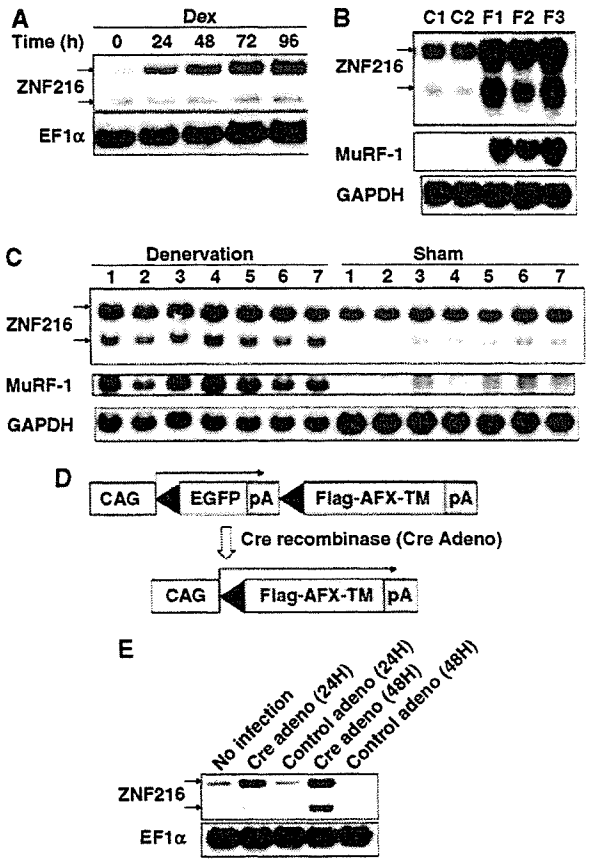

Figure 4 Expression of ZNF216 is induced by muscle atrophy. (**A**) C2C12 myoblast cells were differentiated into myotubes, and treated with 100 μM Dex for the indicated times. Northern blotting was performed to reveal the effect of Dex on ZNF216 expression. The entire coding region of ZNF216 was used as a probe, which recognized 2.4 and 1.5 kb mRNA species arising from alternative splicing and polyadenylation. The loading control was elongation factor α (EF1α). (**B**) Fasting-induced muscle atrophy. Three mice were fasted (F1 ~ F3), and two mice (C1, C2) were fed freely. After 2 days, RNA was purified from gastrocnemius muscle, and Northern blotting was performed to determine ZNF216 expression. The membrane was re-probed with MuRF-1 and GAPDH. (**C**) Denervation-induced muscle atrophy was induced by cutting the sciatic nerve of the hindlimb of seven mice (1 ~ 7). The opposite limb was sham operated as the control. At 7 days after surgery, total RNA was purified from gastrocnemius muscles, and Northern blotting was performed to detect ZNF216 expression. The membrane was re-probed with MuRF-1 and GAPDH. (**D**) Cre-loxP-mediated, constitutively active FOXO expression system. cDNA encoding FLAG-tagged constitutively active FOXO4 (AFX-TM) is separated from the CAG promoter of an expression vector by a loxP-flanked EGFP-poly(A) cassette. Infection with adenovirus expressing Cre recombinase (Cre) results in excision of the DNA fragment located between the two loxP sequences and expression of FLAG-tagged AFX-TM. (**E**) ZNF216 is downstream of FOXO. Total RNAs were prepared from C2C12-AFX-TM cells at the indicated times after infection with adenovirus expressing Cre (Cre) or lacZ (control) and probed by *Znf216* or EF1α. A marked increase in expression of *Znf216* was observed only in Cre-infected cells.

Znf216$^{lex/lex}$ male mice were 42.66 ± 7.06 g ($n = 14$) and 33.16 ± 4.44 g ($n = 9$), respectively. The average weights of female *Znf216*$^{+/+}$ and *Znf216*$^{lex/lex}$ mice were 34.46 ± 4.21 g ($n = 14$) and 26.85 ± 5.38 g ($n = 11$), respectively. After 30 weeks, both female and male *Znf216*$^{lex/lex}$ mice showed no or subtle increases in weight, whereas *Znf216*$^{+/+}$ or

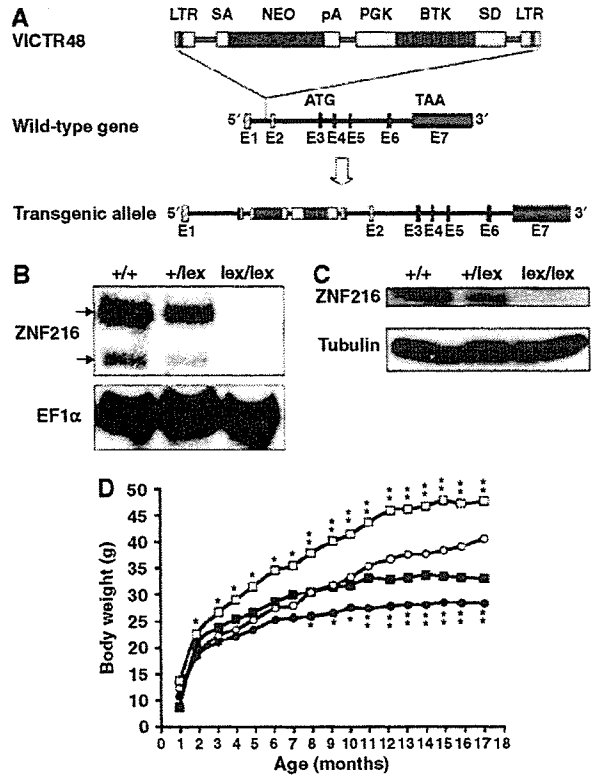

Figure 5 Disruption of *Znf216* gene in mice. (**A**) Gene trap strategy of *Znf216* gene. The structure of the trapping vector, VICTR48, is shown in the upper line. The wild-type allele and the trapped, transgenic allele follow the vector. The retroviral vector, VICTR48, was integrated between exons 1 and 2 of the *Znf216* gene and transcription of downstream exons encoding ZNF216 was diminished. Exons are depicted by striped (noncoding exons) or shadowed boxes (protein-coding exons) and numbered (E1 and E2). LTR, long terminal repeat; SA, splice acceptor site; SD, splice donor site; pA, polyadenylation signal; PGK, PGK promoter. (**B**) Northern blot analysis. Total RNA was prepared from brains of *Znf216*$^{+/+}$, *Znf216*$^{+/lex}$ or *Znf216*$^{lex/lex}$ mice. Full-length mouse ZNF216 cDNA was used as a probe. The membrane was re-probed using an EF1α probe. (**C**) Immunoblot analysis. Extracts from brain of *Znf216*$^{+/+}$, *Znf216*$^{+/lex}$ or *Znf216*$^{lex/lex}$ mice were immunoblotted with antibody against ZNF216. The membrane was re-probed using anti-tubulin antibody. (**D**) Growth curve of *Znf216*$^{lex/lex}$ mice. Body weights at each time point of *Znf216*$^{+/+}$ and *Znf216*$^{lex/lex}$ mice were indicated as open square boxes (males) or circles (females) and closed square boxes (males) or circles (females), respectively. $^{*}P < 0.05$; $^{**}P < 0.005$.

Znf216$^{+/lex}$ mice gained weight as they aged (Figure 5D). The size of most organs in *Znf216*$^{lex/lex}$ mice was reduced in proportion with body weight. However, the fat volume of aged (>30 weeks of age) *Znf216*$^{lex/lex}$ mice was significantly decreased, suggesting that the marked difference in body weight between wild-type and aged *Znf216*$^{lex/lex}$ mice is mainly caused by decreased fat mass seen in *Znf216*$^{lex/lex}$ mice (not shown). Detailed phenotypic characterization of aged mutant mice will be provided elsewhere.

Znf216$^{lex/lex}$ mice exhibit partial resistance to denervation-induced muscle atrophy

To further explore the involvement of ZNF216 in muscle atrophy, neurectomy of sciatic nerve was undertaken in wild-type and *Znf216*$^{lex/lex}$ mice. As shown in Figure 6A, 7

days after denervation, significant muscle weight loss and reduction in fiber sizes of the gastrocnemius muscle were observed in wild-type mice. By contrast, such decreases in muscle weight were significantly attenuated in *Znf216*$^{lex/lex}$ mice (Figure 6A). Sections of gastrocnemius muscle also showed larger fibers in muscle from neurectomized *Znf216*$^{lex/lex}$ mice than in control muscle (Figure 6B). However, there was no significant difference in fiber area between sham-operated wild-type and *Znf216*$^{lex/lex}$ mice (wild type + sham operated, $1988 \pm 530\,\mu m^2$; wild type + denervation, $1379 \pm 345\,\mu m^2$; lex/lex + sham operated, $1776 \pm 484\,\mu m^2$; lex/lex + denervation, $1393 \pm 344\,\mu m^2$). As shown in Figure 6C, the reduction in fiber area was also less apparent in *Znf216*$^{lex/lex}$ mice compared to wild-type mice. These results suggest that ZNF216 plays a crucial role in reduction of muscle mass on denervation-induced muscle atrophy.

Abnormal accumulation of ubiquitinylated proteins in muscle from Znf216$^{lex/lex}$ *mice*

To investigate what abnormalities occur during denervation-induced muscle atrophy in *Znf216*$^{lex/lex}$ mice, we examined

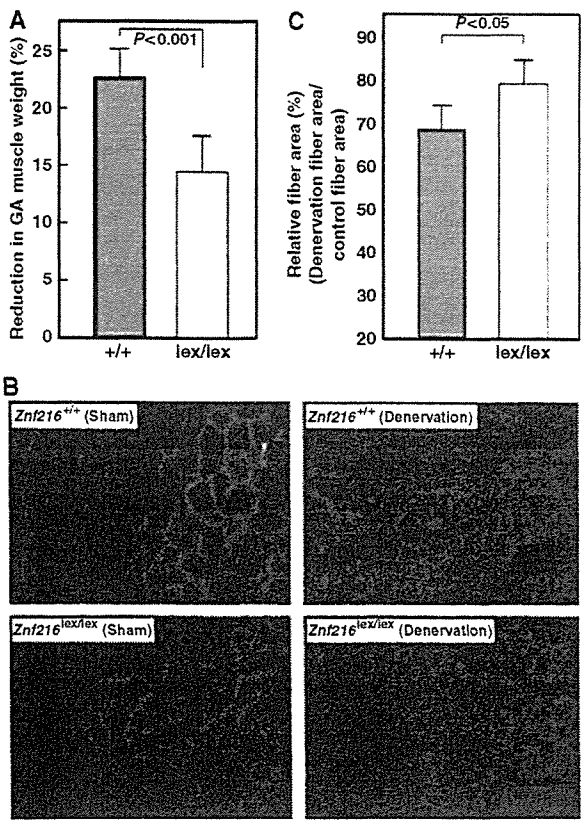

Figure 6 Denervation induced muscular atrophy was attenuated in *ZNF216*$^{lex/lex}$ mice. (**A**) Reduction of GA muscle weight upon neurectomy. Percent decreases in muscle weights are shown as a percent of control, calculated as the left/right muscle weights. (**B**) Cross-sections from gastrocnemius muscle were stained by indirect immunofluorescence with anti-laminin. The reduction in size was also significant in muscle fibers of control mice but less in *Znf216*$^{lex/lex}$. (**C**) Muscle fiber cross-sectional areas were measured in transverse tissue section (B). Percent relative fiber area of denervated muscle to control fiber area (sham-operated) are shown.

expression levels of factors involved in muscle atrophy. As expected, expression of MAFbx/Atrogin-1 and MuRF-1 was dramatically induced by denervation-induced muscle atrophy in gastrocnemius muscle from wild-type mice (Figure 6A). In *Znf216*$^{lex/lex}$ mice, expression of MAFbx/Atrogin-1 and MuRF-1 was also induced at levels comparable to those seen in wild-type mice. Induction of *Pmsa1* and *Pmsd11*, genes encoding the 26S proteasome subunits α6 and Rpn6, respectively, was also indistinguishable between *Znf216*$^{lex/lex}$ and wild-type mice (Figure 7A). Furthermore, proteasome activities in gastrocnemius muscles were comparable between wild-type and *Znf216*$^{lex/lex}$ mice (Figure 7B). Thus, induction of relevant ubiquitin ligases or proteasome components was not affected in *Znf216*$^{lex/lex}$ mice. It is known that ubiquitinylated proteins accumulate during muscle atrophy (Medina *et al*, 1991; Wing *et al*, 1995). As shown in Figure 7C, following denervation, ubiquitinylated proteins accumulated in the gastrocnemius muscle of wild-type mice, but higher levels of ubiquitinylated proteins accumulated in muscle derived from *Znf216*$^{lex/lex}$ mice (~2-fold: $P<0.001$ in neurectomized *Znf216*$^{lex/lex}$ versus wild-type muscle). Similar results were obtained by fasting-induced muscle atrophy, although no difference in the levels of ubiquitinylated proteins from controls (sham-operated or fed) was observed between genotypes (Figure 7C). These results indicate that ZNF216 is a critical regulator of muscle atrophy, most likely functioning to regulate degradation of muscle proteins without altering expression of proteasomal components or known E3 ligases.

Effect of ZNF216 on UPS-mediated protein degradation

Accumulation of ubiquitinylated protein under any circumstance might be because of loss of inhibition of ubiquitinylation and/or deubiquitinylation (DUB). However, no inhibition or DUB activity was observed (Supplementary Figures S4 and S5). As shown in Figure 7D, association of ZNF216 protein to the proteasome was significantly increased when atrophy was induced, suggesting that ZNF216 may be involved in association of ubiquitinylated proteins and the proteasome. The biochemical activity of ZNF216 is similar to that of the UPS proteins, hHR23 and hPLIC, both of which have a shuttle function and are known to bind to both polyubiquitinylated proteins and the 26S proteasome (Hartmann-Petersen and Gordon, 2004; Elsasser and Finley, 2005). Interestingly, overexpression of hHR23 and hPLIC results in stabilization of unstable proteins such as p53 (Kleijnen *et al*, 2000; Glockzin *et al*, 2003). To determine if ZNF216 functioned similarly, we employed a degradation system using unstable GFP (Bence *et al*, 2001). In this system, the CL1 peptide, which functions as a degron, is fused to EGFP (EGFP-CL1). Degradation by conjugation with the degron is mediated by the UPS (Bence *et al*, 2001). EGFP-CL1, constitutively expressed in HEK293 cells, is unstable and the estimated half-life ($t_{1/2}$) of EGFP-CL1 in this system is about 11 min. Ubiquitinylated EGFP-CL1 protein stabilized by treatment with a proteasome inhibitor was associated with ZNF216 but EGFP itself was not (not shown). As shown in Figure 8A, protein degradation was markedly retarded in the presence of ectopic ZNF216 ($t_{1/2}>30$ min) compared to cells transfected with the loss of function mutant ZNF216M3 or mock-transfected cells. Rapid turnover of EGFP-CL1 protein was inhibited by treatment with the

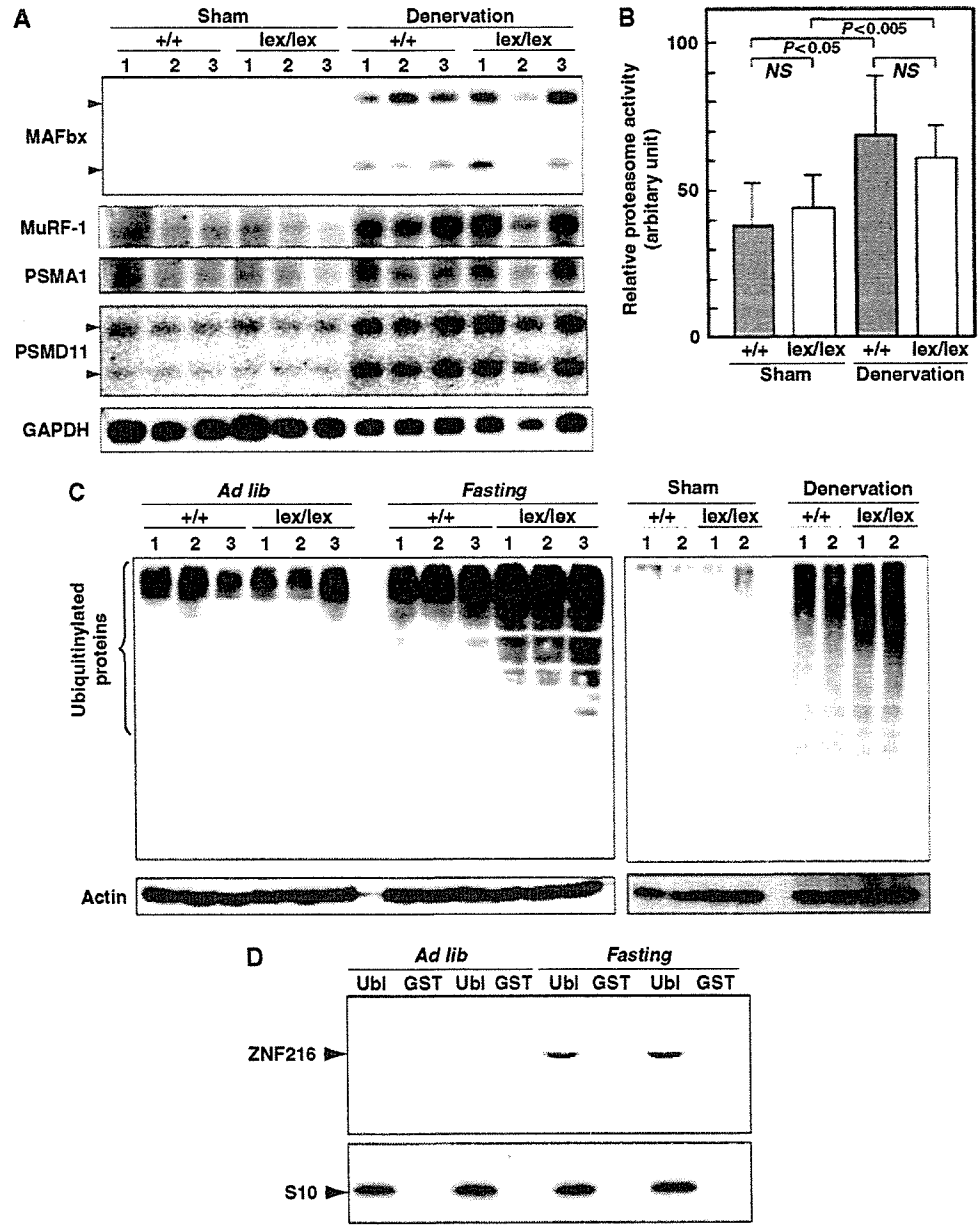

Figure 7 Changes in UPS upon muscular atrophy. (**A**) Expression of UPS components in denervation-induced muscular atrophy. Total RNAs were purified from gastrocnemius muscle, and Northern blotting was performed using indicated probes. Expression of genes for ubiquitin-ligases, such as MAFbx or MuRF-1, and proteasome subunits PSMA1 and PSMD11 was induced by muscle atrophy at comparable levels between wild-type and *ZNF216*$^{lex/lex}$ mice. (**B**) Proteasome activity. Proteasome activities in muscle extracts from wild-type or *ZNF216*$^{lex/lex}$ mice were measured and are shown as arbitrary units. No significant difference in proteasome activity between wild-type and *ZNF216*$^{lex/lex}$ was observed. (**C**) High levels of ubiquitinylated proteins accumulated in muscles from *ZNF216*$^{lex/lex}$ mice than in muscles from wild-type mice. Muscle extracts from wild-type or *ZNF216*$^{lex/lex}$ mice were subjected to immunoblotting using anti-ubiquitin antibody to analyze levels of ubiquitinylated proteins. Left and right panels show fasting-induced and denervation-induced muscle atrophy, respectively. Each membrane was re-probed with anti-actin antibody. (**D**) Association of ZNF216 with the proteasome was increased upon atrophy. The proteasome fractions in muscle extracts from fed (*ad lib*) or fasted (fasting) mice were precipitated with GST-Ubl or GST only as a negative control. Endogenous ZNF216 protein was co-precipitated with the proteasome, which is probed by the anti-S10 antibody.

proteasome inhibitor MG132 (MG132, Figure 8B). The levels of the proteins stabilized by MG132 were comparable among cells transfected with ZNF216 constructs, indicating that protein synthesis of EGFP-CL1 was not significantly affected by ectopic expression of ZNF216 (MG132, Figure 8B). ZNF216WT, and to a lesser extent the mutants M1 and M2 but not M3, attenuated degradation (NT, Figure 8B). Thus, as is the case with other shuttle proteins, overexpression of ZNF216 inhibits degradation of unstable proteins via the UPS.

Discussion

ZNF216 is an atrogene

In this report, we show that *Znf216*$^{lex/lex}$ mice exhibit resistance to denervation-induced muscle atrophy. It has been

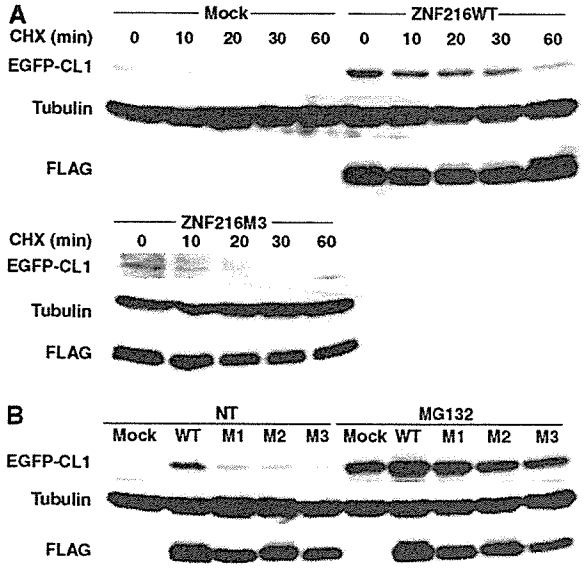

Figure 8 Ectopic expression of ZNF216-affected protein degradation. (**A**) Degradation of EGFP-CL1 protein was delayed by overexpression of ZNF216. 293 cells stably expressing EGFP-CL1 were transfected with plasmid of ZNF216WT, ZNF216M3 or pcDNA3 (mock). Estimated half-lives of the EGFP-CL1 are 35, 11 and 11 min in ZNF216WT-, ZNF216M3- and mock-transfected cells, respectively. *De novo* protein synthesis was arrested by cycloheximide (CHX). The membrane was re-probed with tubulin antibody to control for protein loading (tubulin) and FLAG antibody to detect ZNF216 expression (FLAG). (**B**) Degradation of EGFP-CL1 protein in the presence of various ZNF216 constructs. HEK293 cells stably expressing EGFP-CL1 were transfected with plasmids expressing the indicated mutants. Transfected cells were not treated (NT) or MG132-treated (MG132), and EGFP-CL1 protein was detected with an anti-GFP antibody (EGFP-CL1). The membrane was re-probed with tubulin antibody to control for protein loading (tubulin) and FLAG antibody to detect ZNF216 expression (FLAG).

shown that TNFα induces catabolic conditions through UPS during cancer cachexia (Mitch and Price, 2001). Recently, it has been reported that mice deficient in molecules involved in the NF-κB pathway exhibit resistance to muscular atrophy (Cai *et al*, 2004; Hunter and Kandarian, 2004; McKinnell and Rudnicki, 2004). On the other hand, the IGF-FOXO axis has been suggested to regulate muscle mass through induction of 'atrogenes' such as Murf1 and MAFbx/Atrogin-1 (Sandri *et al*, 2004; Stitt *et al*, 2004). Although we provide evidence that *Znf216* is downstream of FOXO, the NF-κB pathway could represent an alternative signal inducing ZNF216. Indeed, we have identified *Znf216* as a gene induced by RANKL, a TNF family ligand (Hishiya *et al*, 2005) which activates the NF-κB pathway through RANK (Anderson *et al*, 1997; Lacey *et al*, 1998). Moreover, TNFα and IL-1β upregulate expression of ZNF216 in fibroblasts and macrophages (Hishiya *et al*, 2005). These results suggest that *Znf216* may be activated by NF-κB. Huang *et al* (2004) recently reported that ZNF216 inhibits the NF-κB pathway. Whereas treatment with TNFα or overexpression of TRAF6 dramatically activated a reporter driven by NF-κB response elements, ectopic expression of A20/TNFAIP3 but not ZNF216 inhibited NF-κB activation (not shown). Using mouse embryonic fibroblasts, splenocytes or bone marrow cells from $Znf216^{lex/lex}$ or wild-type mice, no significant differences were observed in TNFα-dependent NF-κB activation, LPS-induced cytokine expression or proliferation (unpublished data). Therefore, ZNF216 seems to function as a downstream effector (i.e., a component of the UPS) rather than a specific negative regulator of NF-κB signaling, although ZNF216 function in that pathway is still under investigation. Whereas expression of ZNF216 is not restricted to muscle, such expression was induced upon muscular atrophy and loss of function of *Znf216* promotes resistance to denervation-induced atrophy, thereby suggesting that it fulfills the definition of an 'atrogene'.

As it is in skeletal muscle, ZNF216 is highly expressed in the brain (Scott *et al*, 1998). Aberrations in the UPS have been documented in the pathogenesis of neurodegenerative diseases such as Parkinson's and Huntington's diseases (Ross and Poirier, 2004). Massive accumulation of ubiquitinylated proteins, which are often aggregated and impair the UPS leading to neuronal degeneration, has been observed in these pathogenic conditions (Ciechanover and Brundin, 2003; Korhonen and Lindholm, 2004). In cultured cells, blocking the UPS by proteasome inhibitors leads to accumulation of ubiquitinylated proteins. These ubiquitinylated proteins are then transferred to perinuclear locations and form aggresomes (Johnston *et al*, 1998). As shown here, ZNF216 is localized in aggresomes together with ubiquitinylated proteins. Interestingly, proteomic analysis of a protein complex containing HDAC6, a protein often associated with aggresomes (Kawaguchi *et al*, 2003), showed that the complex included AWP1, a structural homologue of ZNF216 (Seigneurin-Berny *et al*, 2001). Although it is unclear whether ZNF216 is involved in aggresome formation, there is great interest in the role of ZNF216 in the pathogenesis of neurodegenerative diseases.

Molecular function of an A20-containing protein, ZNF216

In muscle atrophy, more ubiquitinylated proteins accumulate in muscle from $Znf216^{lex/lex}$ mice than in muscle from wild-type mice, suggesting an abnormal UPS function. Inhibition of neither polyubiquitinylation nor DUB activity was observed in ZNF216. Although our *in vivo* data showed significant accumulation of polyubiquitinylated proteins in muscle from $Znf216^{lex/lex}$ mice, there is a possibility that ZNF216 is a ubiquitin-ligase. It has been recently reported that A20/TNFAIP3 protein possesses ubiquitin ligase activity against RIP through its ZnF-A20 repeats (Wertz *et al*, 2004). We asked whether the ZnF-A20 of ZNF216 exhibited activity similar to A20/TNFAIP3, but *in vitro* ubiquitinylation assays were negative (Supplementary Figure S6). In fact, the ZnF-A20 of A20/TNFAIP3 protein does not bind polyubiquitin chains as does the ZnF-A20 of ZNF216 (Supplementary Figure S1). Furthermore, there are seven ZnF-A20 motifs in A20/TNFAIP3 and only the fourth is responsible for E3 activity, suggesting that the ZnF-A20 motif is not inherently active enzymatically (Wertz *et al*, 2004). However, we cannot exclude the possibility that ZNF216 may possess DUB or E3 activity highly specific to an unknown substrate without nonspecific or self-ubiquitinylating activity.

ZNF216 likely acts as a bridging or a shuttle factor of ubiquitinylated proteins targeted to the proteasome. Shuttle proteins, such as Rad23p and Dsk2p, share interfaces for ubiquitinylated proteins and the proteasome (Hartmann-Petersen and Gordon, 2004; Elsasser and Finley, 2005).

Although shuttle proteins are required for efficient protein degradation, ectopic expression of hHR23 or hPLIC, the human homologues of Rad23p or Dsk2p, respectively, lead to stabilization of p53 protein (Kleijnen *et al*, 2000; Glockzin *et al*, 2003). These outcomes may be caused by titration effects due to overexpression and are commonly observed following misexpression of shuttle proteins in yeast and mammals (Hartmann-Petersen and Gordon, 2004; Verma *et al*, 2004). Here, we show that ZNF216 has a ubiquitin binding domain and can associate with the 26S proteasome even in the absence of ubiquitin binding, and that overexpression of the zinc-finger protein attenuates protein degradation rate. There is no structural counterpart of ZNF216 in the yeast genome. We asked whether ZNF216 could rescue the bridging function of RAD23 or DSK2 mutants by introducing ZNF216 into *Δrad23Δdsk2* yeast cells, but the phenotype could not be rescued (data not shown). This suggests that ZNF216 is not the functional orthologue of these proteins. Recently, the presence of an alternative pathway of Rad23p/Dsk2p in protein targeting to the proteasome has been suggested (Bazirgan and Hampton, 2005; Richly *et al*, 2005). It has been reported that tetra-ubiquitin constitutes the minimum proteasomal targeting signal and that the length of polyubiquitin chain may determine the targeting route (Thrower *et al*, 2000; Bazirgan and Hampton, 2005; Richly *et al*, 2005). Notably, ZNF216 preferentially binds polyubiquitin chains longer than di- or tri-ubiquitin (Figure 1D). Therefore, these data suggest that ZNF216 is a novel ubiquitin recognition factor, required for efficient protein degradation via a pathway different from the canonical Rad23p/Dsk2p pathway. Although it is now under investigation, the characterization of ZnF-AN1, an AN1-type zinc-finger domain located at the C-terminus of ZNF216, may reveal the precise molecular function of ZNF216.

Materials and methods

Antibodies

An anti-ZNF216 antibody was raised by immunizing rabbits against synthesized peptide corresponding to the C-terminal sequence of mouse ZNF216. Mouse monoclonal antibodies for FLAG (Sigma, St Louis, MO) and ubiquitin (Santa Cruz Biotechnology, CA), rabbit polyclonal antibodies for ubiquitin (Affiniti Research Products) and actin (Neo Markers, CA), a rat monoclonal antibody for HA (Roche Diagnostics, Mannheim, Germany), and a rabbit polyclonal antibody against S10a/Rpn7p (Affiniti Research Products) were purchased from the indicated manufacturers. For indirect immunofluorescence staining, AlexaFluor 488 goat anti-mouse IgG or AlexaFluor 546 goat anti-rat IgG antibody was obtained from Molecular Probes, OR.

Identification of interacting proteins

RNA was purified from RAW264.7 cells stimulated by RANKL, and used to construct the yeast library (MatchMaker Library Construction & Screening Kit, Clontech). Yeast two-hybrid screening with pGBKT7-ZNF216 was performed as described previously (Masuda *et al*, 2001). Identification of the co-immunoprecipitated proteins with N- or C-terminally FLAG-tagged ZNF216 (ZA20D2) or AWP1 (ZA20D3) was essentially done by a nano-LC/MS/MS system as previously described (Natsume *et al*, 2002; Komatsu *et al*, 2004).

Experimental models of muscle atrophy

For fasting-induced muscle atrophy, 8-week-old C57BL6 male mice were deprived of food but given free access to water. After 2 days, gastrocnemius muscles were harvested for each experiment. Denervation-induced muscle atrophy was performed by dissecting the sciatic nerve of one hindlimb, and the other hindlimb was sham operated as the control. After 7 days, the contralateral normal and denervated gastrocnemius muscles were harvested for each experiment. All animal experiments were approved in advance by the Ethics Review Committee for Animal Experimentation of the National Institute for Longevity Sciences and the National Center for Geriatrics and Gerontology. Student's *t*-tests were used to evaluate statistical differences between the two groups.

Znf216-deficient mice

Generation of heterozygous *Znf216*$^{+/lex}$ mice was essentially done by the gene trap method at Lexicon Genetics (Zambrowicz *et al*, 1998). Briefly, ES cells heterozygous for the trapped *Znf216* gene were microinjected into eight-cell-stage ICR mouse embryos and transplanted into uteri. Chimeric mice were crossed to C57BL/6J mice. Northern and immunoblot analyses confirmed disruption of the gene (see text). For genotyping, primers were as follows: KO-A, ACCGACAGGATAGACAATGGCAGAG; KO-B, CGATTTTAAGAAAG GAGGCTCTGACC; LTR2, AAATGGCGTTACTTAAGCTAGCTTGC. The wild-type and inserted alleles were detected by PCR using KO-A and KO-B (0.5 kb), and LTR2 and KO-B (0.3 kb), respectively.

EGFP-CL1 degradation assay

The nucleotide sequence encoding the CL1 peptide (ACKNWFSSLSHFVIHL) (Gilon *et al*, 1998) was inserted into the *Xho*I/*Eco*RI site of pEGFP-C3, and the resulting plasmid was designated pEGFP-CL1. A cell line stably expressing EGFP-CL1 (293EGFP-CL1) was generated by transfection of pEGFP-CL1 into 293 cells. For the degradation assay, ZNF216 expression vectors were transfected into 293EGFP-CL1 cells and cells were harvested 48 h after transfection. MG132 (final 10 μM) or cycloheximide (final 100 μg/ml) was added to the culture at 12 or 1 h before harvest, respectively. Protein extraction was as described above.

For more details on supplementary Materials and methods, see Supplementary data

Supplementary data

Supplementary data are available at *The EMBO Journal* Online.

Acknowledgements

We are grateful to Drs Kazuhiro Iwai (Osaka City University) and Noboru Motoyama (NCGG) for reagents, helpful comments and suggestions throughout this study. We also thank Drs Akio Matsuda and Tatsuo Furuyama for experimental instruction and advice; Dr Aya Sasaki for pathological determinations; Ms Miho Kamiya and Ms Kumi Tsutsumi for technical assistance; and Dr Elise Lamar for proofreading the manuscript. This study is supported in part by the Program for Promotion of Fundamental Studies in Health Sciences of the Organization for Pharmaceutical Safety and Research of Japan, and by a Research Grant for Longevity Sciences from the Ministry of Health, Labor and Welfare.

References

Anderson DM, Maraskovsky E, Billingsley WL, Dougall WC, Tometsko ME, Roux ER, Teepe MC, DuBose RF, Cosman D, Galibert L (1997) A homologue of the TNF receptor and its ligand enhance T-cell growth and dendritic-cell function. *Nature* **390:** 175–179

Bailey JL, Wang X, England BK, Price SR, Ding X, Mitch WE (1996) The acidosis of chronic renal failure activates muscle proteolysis in rats by augmenting transcription of genes encoding proteins of the ATP-dependent ubiquitin-proteasome pathway. *J Clin Invest* **97:** 1447–1453

Bazirgan OA, Hampton RY (2005) Cdc48-Ufd2-Rad23: the road less ubiquitinated? *Nat Cell Biol* **7:** 207–209

Bence NF, Sampat RM, Kopito RR (2001) Impairment of the ubiquitin–proteasome system by protein aggregation. *Science* **292:** 1552–1555

protein gene at the DFNB7/11 and dn hearing-loss loci on human chromosome 9q and mouse chromosome 19. *Gene* **215:** 461–469

Seigneurin-Berny D, Verdel A, Curtet S, Lemercier C, Garin J, Rousseaux S, Khochbin S (2001) Identification of components of the murine histone deacetylase 6 complex: link between acetylation and ubiquitination signaling pathways. *Mol Cell Biol* **21:** 8035–8044

Stitt TN, Drujan D, Clarke BA, Panaro F, Timofeyva Y, Kline WO, Gonzalez M, Yancopoulos GD, Glass DJ (2004) The IGF-1/PI3K/Akt pathway prevents expression of muscle atrophy-induced ubiquitin ligases by inhibiting FOXO transcription factors. *Mol Cell* **14:** 395–403

Tawa Jr NE, Odessey R, Goldberg AL (1997) Inhibitors of the proteasome reduce the accelerated proteolysis in atrophying rat skeletal muscles. *J Clin Invest* **100:** 197–203

Thrower JS, Hoffman L, Rechsteiner M, Pickart CM (2000) Recognition of the polyubiquitin proteolytic signal. *EMBO J* **19:** 94–102

Verma R, Oania R, Graumann J, Deshaies RJ (2004) Multiubiquitin chain receptors define a layer of substrate selectivity in the ubiquitin–proteasome system. *Cell* **118:** 99–110

Wertz IE, O'Rourke KM, Zhou H, Eby M, Aravind L, Seshagiri S, Wu P, Wiesmann C, Baker R, Boone DL, Ma A, Koonin EV, Dixit VM (2004) De-ubiquitination and ubiquitin ligase domains of A20 downregulate NF-kappaB signalling. *Nature* **430:** 694–699

Wilkinson CR, Ferrell K, Penney M, Wallace M, Dubiel W, Gordon C (2000) Analysis of a gene encoding Rpn10 of the fission yeast proteasome reveals that the polyubiquitin-binding site of this subunit is essential when Rpn12/Mts3 activity is compromised. *J Biol Chem* **275:** 15182–15192

Wing SS, Goldberg AL (1993) Glucocorticoids activate the ATP-ubiquitin-dependent proteolytic system in skeletal muscle during fasting. *Am J Physiol* **264:** E668–E676

Wing SS, Haas AL, Goldberg AL (1995) Increase in ubiquitin–protein conjugates concomitant with the increase in proteolysis in rat skeletal muscle during starvation and atrophy denervation. *Biochem J* **307** (Part 3): 639–645

Young P, Deveraux Q, Beal RE, Pickart CM, Rechsteiner M (1998) Characterization of two polyubiquitin binding sites in the 26 S protease subunit 5a. *J Biol Chem* **273:** 5461–5467

Zambrowicz BP, Friedrich GA, Buxton EC, Lilleberg SL, Person C, Sands AT (1998) Disruption and sequence identification of 2000 genes in mouse embryonic stem cells. *Nature* **392:** 608–611

Bodine SC, Latres E, Baumhueter S, Lai VK, Nunez L, Clarke BA, Poueymirou WT, Panaro FJ, Na E, Dharmarajan K, Pan ZQ, Valenzuela DM, DeChiara TM, Stitt TN, Yancopoulos GD, Glass DJ (2001) Identification of ubiquitin ligases required for skeletal muscle atrophy. *Science* **294:** 1704–1708

Brunet A, Bonni A, Zigmond MJ, Lin MZ, Juo P, Hu LS, Anderson MJ, Arden KC, Blenis J, Greenberg ME (1999) Akt promotes cell survival by phosphorylating and inhibiting a Forkhead transcription factor. *Cell* **96:** 857–868

Cai D, Frantz JD, Tawa Jr NE, Melendez PA, Oh BC, Lidov HG, Hasselgren PO, Frontera WR, Lee J, Glass DJ, Shoelson SE (2004) IKKbeta/NF-kappaB activation causes severe muscle wasting in mice. *Cell* **119:** 285–298

Chen L, Shinde U, Ortolan TG, Madura K (2001) Ubiquitin-associated (UBA) domains in Rad23 bind ubiquitin and promote inhibition of multi-ubiquitin chain assembly. *EMBO Rep* **2:** 933–938

Ciechanover A, Brundin P (2003) The ubiquitin proteasome system in neurodegenerative diseases: sometimes the chicken, sometimes the egg. *Neuron* **40:** 427–446

Elsasser S, Finley D (2005) Delivery of ubiquitinated substrates to protein-unfolding machines. *Nat Cell Biol* **7:** 742–749

Funakoshi M, Sasaki T, Nishimoto T, Kobayashi H (2002) Budding yeast Dsk2p is a polyubiquitin-binding protein that can interact with the proteasome. *Proc Natl Acad Sci USA* **99:** 745–750

Furukawa-Hibi Y, Yoshida-Araki K, Ohta T, Ikeda K, Motoyama N (2002) FOXO forkhead transcription factors induce G(2)-M checkpoint in response to oxidative stress. *J Biol Chem* **277:** 26729–26732

Gilon T, Chomsky O, Kulka RG (1998) Degradation signals for ubiquitin system proteolysis in Saccharomyces cerevisiae. *EMBO J* **17:** 2759–2766

Glickman MH, Ciechanover A (2002) The ubiquitin-proteasome proteolytic pathway: destruction for the sake of construction. *Physiol Rev* **82:** 373–428

Glockzin S, Ogi FX, Hengstermann A, Scheffner M, Blattner C (2003) Involvement of the DNA repair protein hHR23 in p53 degradation. *Mol Cell Biol* **23:** 8960–8969

Gomes MD, Lecker SH, Jagoe RT, Navon A, Goldberg AL (2001) Atrogin-1, a muscle-specific F-box protein highly expressed during muscle atrophy. *Proc Natl Acad Sci USA* **98:** 14440–14445

Hartmann-Petersen R, Gordon C (2004) Protein degradation: recognition of ubiquitinylated substrates. *Curr Biol* **14:** R754–R756

Hershko A, Ciechanover A (1998) The ubiquitin system. *Annu Rev Biochem* **67:** 425–479

Hishiya A, Ikeda K, Watanabe K (2005) A RANKL-inducible gene Znf216 in osteoclast differentiation. *J. Receptor Signal Transduct* **25:** 199–216

Horiuchi H, Lippe R, McBride HM, Rubino M, Woodman P, Stenmark H, Rybin V, Wilm M, Ashman K, Mann M, Zerial M (1997) A novel Rab5 GDP/GTP exchange factor complexed to Rabaptin-5 links nucleotide exchange to effector recruitment and function. *Cell* **90:** 1149–1159

Huang J, Teng L, Li L, Liu T, Li L, Chen D, Xu LG, Zhai Z, Shu HB (2004) ZNF216 is an A20-like and IkappaB kinase gamma-interacting inhibitor of NFkappaB activation. *J Biol Chem* **279:** 16847–16853

Hunter RB, Kandarian SC (2004) Disruption of either the Nfkb1 or the Bcl3 gene inhibits skeletal muscle atrophy. *J Clin Invest* **114:** 1504–1511

Jagoe RT, Lecker SH, Gomes M, Goldberg AL (2002) Patterns of gene expression in atrophying skeletal muscles: response to food deprivation. *FASEB J* **16:** 1697–1712

Johnston JA, Ward CL, Kopito RR (1998) Aggresomes: a cellular response to misfolded proteins. *J Cell Biol* **143:** 1883–1898

Kawaguchi Y, Kovacs JJ, McLaurin A, Vance JM, Ito A, Yao TP (2003) The deacetylase HDAC6 regulates aggresome formation and cell viability in response to misfolded protein stress. *Cell* **115:** 727–738

Kleijnen MF, Shih AH, Zhou P, Kumar S, Soccio RE, Kedersha NL, Gill G, Howley PM (2000) The hPLIC proteins may provide a link between the ubiquitination machinery and the proteasome. *Mol Cell* **6:** 409–419

Komatsu M, Chiba T, Tatsumi K, Iemura S, Tanida I, Okazaki N, Ueno T, Kominami E, Natsume T, Tanaka K (2004) A novel protein-conjugating system for Ufm1, a ubiquitin-fold modifier. *EMBO J* **23:** 1977–1986

Kopito RR (2000) Aggresomes, inclusion bodies and protein aggregation. *Trends Cell Biol* **10:** 524–530

Korhonen L, Lindholm D (2004) The ubiquitin proteasome system in synaptic and axonal degeneration: a new twist to an old cycle. *J Cell Biol* **165:** 27–30

Lacey DL, Timms E, Tan HL, Kelley MJ, Dunstan CR, Burgess T, Elliott R, Colombero A, Elliott G, Scully S, Hsu H, Sullivan J, Hawkins N, Davy E, Capparelli C, Eli A, Qian YX, Kaufman S, Sarosi I, Shalhoub V, Senaldi G, Guo J, Delaney J, Boyle WJ (1998) Osteoprotegerin ligand is a cytokine that regulates osteoclast differentiation and activation. *Cell* **93:** 165–176

Lambertson D, Chen L, Madura K (1999) Pleiotropic defects caused by loss of the proteasome-interacting factors Rad23 and Rpn10 of *Saccharomyces cerevisiae*. *Genetics* **153:** 69–79

Lecker SH, Jagoe RT, Gilbert A, Gomes M, Baracos V, Bailey J, Price SR, Mitch WE, Goldberg AL (2004) Multiple types of skeletal muscle atrophy involve a common program of changes in gene expression. *FASEB J* **18:** 39–51

Lecker SH, Solomon V, Mitch WE, Goldberg AL (1999) Muscle protein breakdown and the critical role of the ubiquitin–proteasome pathway in normal and disease states. *J Nutr* **129:** 227S–237S

Lelouard H, Gatti E, Cappello F, Gresser O, Camosseto V, Pierre P (2002) Transient aggregation of ubiquitinated proteins during dendritic cell maturation. *Nature* **417:** 177–182

Masuda Y, Sasaki A, Shibuya H, Ueno N, Ikeda K, Watanabe K (2001) Dlxin-1, a novel protein that binds Dlx5 and regulates its transcriptional function. *J Biol Chem* **276:** 5331–5338

McKinnell IW, Rudnicki MA (2004) Molecular mechanisms of muscle atrophy. *Cell* **119:** 907–910

Medina R, Wing SS, Haas A, Goldberg AL (1991) Activation of the ubiquitin-ATP-dependent proteolytic system in skeletal muscle during fasting and denervation atrophy. *Biomed Biochim Acta* **50:** 347–356

Mitch WE, Goldberg AL (1996) Mechanisms of muscle wasting. The role of the ubiquitin-proteasome pathway. *N Engl J Med* **335:** 1897–1905

Mitch WE, Price SR (2001) Transcription factors and muscle cachexia: is there a therapeutic target? *Lancet* **357:** 734–735

Natsume T, Yamauchi Y, Nakayama H, Shinkawa T, Yanagida M, Takahashi N, Isobe T (2002) A direct nanoflow liquid chromatography-tandem mass spectrometry system for interaction proteomics. *Anal Chem* **74:** 4725–4733

Opipari Jr AW, Boguski MS, Dixit VM (1990) The A20 cDNA induced by tumor necrosis factor alpha encodes a novel type of zinc finger protein. *J Biol Chem* **265:** 14705–14708

Pickart CM, Cohen RE (2004) Proteasomes and their kin: proteases in the machine age. *Nat Rev Mol Cell Biol* **5:** 177–187

Price SR, Bailey JL, Wang X, Jurkovitz C, England BK, Ding X, Phillips LS, Mitch WE (1996) Muscle wasting in insulinopenic rats results from activation of the ATP-dependent, ubiquitin-proteasome proteolytic pathway by a mechanism including gene transcription. *J Clin Invest* **98:** 1703–1708

Richly H, Rape M, Braun S, Rumpf S, Hoege C, Jentsch S (2005) A series of ubiquitin binding factors connects CDC48/p97 to substrate multiubiquitylation and proteasomal targeting. *Cell* **120:** 73–84

Ross CA, Poirier MA (2004) Protein aggregation and neurodegenerative disease. *Nat Med* **10** (Suppl): S10–S17

Sacheck JM, Ohtsuka A, McLary SC, Goldberg AL (2004) IGF-I stimulates muscle growth by suppressing protein breakdown and expression of atrophy-related ubiquitin ligases, atrogin-1 and MuRF1. *Am J Physiol Endocrinol Metab* **287:** E591–E601

Saeki Y, Saitoh A, Toh-e A, Yokosawa H (2002) Ubiquitin-like proteins and Rpn10 play cooperative roles in ubiquitin-dependent proteolysis. *Biochem Biophys Res Commun* **293:** 986–992

Sandri M, Sandri C, Gilbert A, Skurk C, Calabria E, Picard A, Walsh K, Schiaffino S, Lecker SH, Goldberg AL (2004) Foxo transcription factors induce the atrophy-related ubiquitin ligase atrogin-1 and cause skeletal muscle atrophy. *Cell* **117:** 399–412

Scott DA, Greinwald Jr JH, Marietta JR, Drury S, Swiderski RE, Vinas A, DeAngelis MM, Carmi R, Ramesh A, Kraft ML, Elbedour K, Skworak AB, Friedman RA, Srikumari Srisailapathy CR, Verhoeven K, Van Gamp G, Lovett M, Deininger PL, Batzer MA, Morton CC, Keats BJ, Smith RJ, Sheffield VC (1998) Identification and mutation analysis of a cochlear-expressed, zinc finger

Dok-3 sequesters Grb2 and inhibits the Ras-Erk pathway downstream of protein-tyrosine kinases

Miyuki Honma[1], Osamu Higuchi[1], Masaki Shirakata[1], Tomoharu Yasuda[1,a] Hiroshi Shibuya[2], Shun-ichiro Iemura[3], Tohru Natsume[3] and Yuji Yamanashi[1,*]

[1]*Departments of Cell Regulation, and [2]Department of Molecular Cell Biology, Medical Research Institute, Tokyo Medical and Dental University, Tokyo 113-8510, Japan*

[3]*National Institutes of Advanced Industrial Science and Technology, Biological Information Research Center, Tokyo 135-0064, Japan*

Adaptor proteins are essential in coordinating recruitment and, in a few cases, restraint of various effectors during cellular signaling. Dok-1, Dok-2 and Dok-3 comprise a closely related family of adaptor, which negatively regulates mitogen-activated protein kinase Erk downstream of protein-tyrosine kinases (PTKs). Recruitment of p120 rasGAP, a potent inhibitor of Ras, by Dok-1 and Dok-2 appears critical in the negative regulation of the Ras-Erk pathway. However, as Dok-3 does not bind rasGAP, it has been unclear how Dok-3 inhibits Erk downstream of PTKs. Here, we identified Grb2 as a Dok-3-binding protein upon its tyrosine phosphorylation. This interaction required the intact binding motifs of the Grb2 SH2 domain, and a mutant (Dok-3-FF) having a Tyr/Phe substitution at these motifs failed to inhibit Ras and Erk activation downstream of a cytoplasmic PTK Src. Because Grb2 forms a stable complex with Sos, a crucial activator of Ras, these data suggest that Dok-3 restrains Grb2 and inhibits the ability of the Grb2-Sos complex to activate Ras. Indeed, forced expression of Dok-3, but not Dok-3-FF, inhibited the recruitment of the Grb2-Sos complex to Shc downstream of Src, which is an essential event for activation of the Ras-Erk pathway. These findings indicate that Dok-3 sequesters Grb2 from Shc and inhibits the Ras-Erk pathway downstream of PTKs.

Introduction

Activation of protein-tyrosine kinases (PTKs) induces tyrosine phosphorylation of target proteins, which triggers inter- or intra-molecular interactions of proteins (Hubbard & Till 2000). Many such interactions are essential in regulation of various cell activities such as proliferation, differentiation, motility, metabolism, and survival. Although PTKs initiate a wide range of positive signaling cascades, they also evoke negative signaling to avoid inappropriate activation of cells, which may cause abnormalities such as malignancies, developmental disorders, metabolic syndromes, chronic inflammation, or autoimmune reactions. The Ras-Erk pathway is one of the positive signaling cascades that are critical in cell activation downstream of PTKs. An enormous number of studies have revealed that Ras activity is regulated by a balance between positive and negative regulators, which are guanine nucleotide exchange factors (GEFs) and GTPase activating proteins (GAPs), respectively (Lowy *et al.* 1991). For example, the GEFs include Sos and the GAPs include p120 rasGAP. An adaptor protein Grb2 is comprised of a central Src homology 2 (SH2) domain and two flanking Src homology 3 (SH3) domains, and it forms a stable complex with Sos via the SH3 domains, thereby linking recruitment of Grb2 to activation of Ras. As the SH2 domain of Grb2 recognizes a phosphotyrosine (pY)-containing motif of the form pYXN (Kessels *et al.* 2002), many PTKs activate the Ras-Erk pathway by recruiting Grb2 to the motifs of their own or downstream adaptors such as Shc. Furthermore, studies with dominant negative mutants, gene targeting, or siRNA-based knock-down of Shc have revealed a critical role for it in activation of the Ras-Erk pathway downstream of PTKs including epidermal growth factor receptor, platelet-derived growth factor (PDGF) receptor, and a cytoplasmic PTK

Communicated by: Tadashi Yamamoto
**Correspondence*: E-mail: yamanashi.creg@mri.tmd.ac.jp
[a]*Present address*: Laboratory for Lymphocyte Differentiation, RIKEN Research Center for Allergy and Immunology, Kanagawa 230-0045, Japan.

DOI: 10.1111/j.1365-2443.2006.00926.x

Src (Lai & Pawson 2000; Ravichandran 2001; Faisal *et al.* 2004).

Dok-1 was originally identified as $p62^{dok}$ that is a common substrate of many PTKs (Carpino *et al.* 1997; Yamanashi & Baltimore 1997). Later, Dok-3 was identified as the third member of the Dok-family of proteins (Cong *et al.* 1999; Lemay *et al.* 2000), which have been expanded to six members, Dok-1 to Dok-6, to date (Di Cristofano *et al.* 1998; Nelms *et al.* 1998; Grimm *et al.* 2001; Crowder *et al.* 2004). These proteins work as adaptors in a variety of signaling situations and share structural similarities characterized by N-terminal pleckstrin homology (PH) and phosphotyrosine binding (PTB) domains (Veillette *et al.* 2002), followed by C-terminal SH2-target sites. The PH domain is involved in lipid-protein interactions and indeed Dok-1 translocated to the plasma membrane upon PDGF-treatment of cells in a manner dependent on phosphoinositide (PI)-3-kinase, which facilitated production of 3′-phosphorylated PIs that are binding targets of the Dok-1 PH domain (Zhao *et al.* 2001). The PTB domain is involved in binding to a phosphotyrosine-containing motif of the form NPXpY or the like and is important for interaction of the Dok-family adaptors with upstream PTKs (Songyang *et al.* 2001; Jones & Dumont 1999). Upon tyrosine phosphorylation of the C-terminal SH2-target motifs, the Dok-family proteins bind or recruit SH2-containing molecules (Yamanashi & Baltimore 1997; Van Slyke *et al.* 2005; Robson *et al.* 2004). Among the Dok-family adaptors, Dok-1, Dok-2 and Dok-3 comprise a closely related subfamily, and forced expression of each of these adaptors in cultured cells negatively regulates Erk downstream of PTKs (Cong *et al.* 1999; Jones & Dumont 1999; Wick *et al.* 2001; Van Slyke *et al.* 2005). Experiments with mice lacking Dok-1 and/or Dok-2 demonstrated an indispensable role for the Dok proteins in negative regulation of the Ras-Erk pathway *in vivo* (Yamanashi *et al.* 2000; Niki *et al.* 2004; Yasuda *et al.* 2004; Shinohara *et al.* 2005). In contrast, biological and biochemical functions of Dok-4, Dok-5 and Dok-6 are still controversial (Grimm *et al.* 2001; Cai *et al.* 2003; Crowder *et al.* 2004). Recently, two research groups including ours independently found that Dok-1 and Dok-2 are key negative regulators of cytokine responses and are essential for myeloid homeostasis and suppression of leukemia in living animals (Niki *et al.* 2004; Yasuda *et al.* 2004). We also found that the Dok-family adaptors negatively regulate Toll-like receptor 4 signaling and are essential for homeostasis of the innate immunity to endotoxin, a bacterial lipopolysaccharide (Shinohara *et al.* 2005).

Since Dok-1 and Dok-2 bind p120 rasGAP upon their tyrosine phosphorylation, these adaptors appear to recruit it as an effector to suppress the Ras-Erk pathway (Nelms *et al.* 1998; Wick *et al.* 2001). Indeed, Dok-1 mutants lacking tyrosine residues responsible for the rasGAP binding have lost these inhibitory effects. However, we previously found that rasGAP binding is not sufficient for the inhibitory function of Dok-1 and others have even reported that it is dispensable for suppression of Erk downstream of the PDGF receptor (Zhao *et al.* 2001; Shinohara *et al.* 2004), suggesting an as yet unidentified mechanism. In fact, Dok-3 does not have a rasGAP-binding motif and does not bind p120 rasGAP. It has recently been reported that forced expression of Dok-3 in a B cell line inhibited production of interleukin-2 upon B cell receptor stimulation, probably by recruiting the lipid phosphatase SHIP (Robson *et al.* 2004). In the particular signaling context discussed here, Dok-3 specifically suppressed activation of JNK but not other effector molecules, including Erk. However, given that forced expression of Dok-3 in 293 cells inhibits Erk activation downstream of PTKs (Cong *et al.* 1999), the molecular mechanism underlying the inhibition of Erk has to be studied. It should also be noted that, unlike Dok-1 and Dok-2, it has been unclear whether Dok-3 inhibits Ras.

Here, we first revealed that forced expression Dok-3 in 293T cells inhibits Ras downstream of Src. To address the mechanism of Dok-3 function, we hypothesized that it interacts with critical regulators of the Ras-Erk pathway besides p120 rasGAP. Thus, we examined proteins that bind Dok-3 upon its tyrosine phosphorylation and found that it is Grb2 that binds Dok-3 in the presence, but not in the absence, of Src. Furthermore, a Dok-3 mutant having a Tyr/Phe substitution in the predicted binding motifs of the Grb2 SH2 domain has lost both its binding activity to Grb2 and its inhibitory effects against Ras and Erk. That forced expression of Dok-3, but not the mutant, inhibited recruitment of the Grb2-Sos complex to Shc downstream of Src indicates that Dok-3 sequesters Grb2 from Shc. Because the recruitment of Grb2-Sos complex to Shc is essential for activation of the Ras-Erk pathway downstream of PTKs, including Src, our findings taken together reveal a novel mechanism in negative regulation of this pathway by the Dok family of adaptors.

Results

Dok-3 suppresses Src-induced activation of Ras

It was previously shown that forced expression of Dok-3 inhibits Erk activation downstream of v-Abl, a constitutively active PTK, but does not inhibit it downstream of a constitutively active form of Ras (Cong *et al.* 1999).

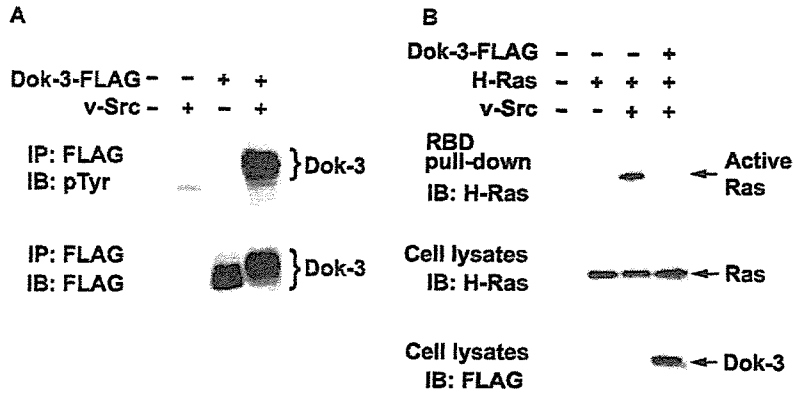

Figure 1 Dok-3 negatively regulates Ras downstream of Src. (A) Forced expression of v-Src phosphorylates Dok-3. 293T cells were transfected with expression plasmids for the indicated proteins, and anti-FLAG immunoprecipitates (IP) were subjected to immunoblotting (IB) with antibodies to phosphotyrosine (pTyr) or FLAG epitope. (B) Forced expression of Dok-3 inhibits activation of Ras. 293T cells were transfected with expression plasmids for the indicated proteins, and whole cell lysates were subjected to RBD pull-down assay for evaluation of activated Ras. Expression levels of H-Ras and Dok-3-FLAG were examined by IB.

Table 1 Proteins associated with Dok-3 in the presence of Src. Molecular mass (m/z) and charge of each peptide ion observed in LC-MS/MS analysis, together with the assigned amino acid sequence and its position in the corresponding protein are shown

Protein	Peptide (m/z)	Charge	Sequence	Residues (start–end)
Grb2	825.74	3	GACHGQTGMFPRNYVTPVNRNV	196–217
	799.35	2	VLNEECDQNWYK	27–38
Csk	558.34	2	GDVLTIVAVTK	33–43
	515.29	3	VGREGIIPANYVQK	54–67
	835.06	3	VMEGTVAAQDEFYRSGWALNMK	172–193
	433.74	2	VSDFGLTK	330–337

This appears to suggest a negative role of Dok-3 between v-Abl and Ras. However, Dok-3 is believed to work as a negative regulator upon its tyrosine phosphorylation, and Ras does not induce such modification, making it difficult to define whether Dok-3 functions upstream of Ras or not. To clarify this, we examined Ras activation downstream of a constitutively active PTK, v-Src, which strongly phosphorylated Dok-3 in 293T cells and slightly decreased its mobility in polyacrylamide gel electrophoresis (Fig. 1A). The Ras-binding domain (RBD) pull-down assay clearly showed that forced expression of Dok-3 in 293T cells inhibits v-Src-mediated activation of Ras (Fig. 1B), indicating that Dok-3 is an upstream regulator of Ras downstream of PTKs. Because Dok-3 does not bind p120 rasGAP, this strongly suggests that Dok-3 interacts with as yet unknown molecules involved in the negative regulation of Ras.

Identification of Grb2 as a Dok-3-binding protein downstream of Src

To identify Dok-3-associated proteins upon its tyrosine phosphorylation, FLAG-tagged Dok-3 was exogenously expressed in 293 cells with or without Src-YF. This mutant is a constitutively active form of Src as it has Tyr/Phe substitution at Tyr-530, which is essential for intramolecular inactivation of catalytic activity. We confirmed that Src-YF strongly phosphorylates Dok-3, as does v-Src, which also lacks the inhibitory tyrosine residue (data not shown). One day after transfection, Dok-3 was immunoprecipitated by agarose-conjugated anti-FLAG antibodies, washed, and eluted with an excess amount of FLAG peptide. The eluted proteins, which included Dok-3 binding partners, were digested with Lys-C endopeptidase (*Achromobacter* protease I) and the cleaved fragments were directly analyzed using the highly sensitive "direct nano-flow LC-MS/MS" system as described in Experimental procedures (Natsume *et al.* 2002; Komatsu *et al.* 2004). Following a database search, a total of six peptides were assigned to MS/MS spectra obtained from four nano-LC-MS/MS analyses for Dok-3-FLAG-associated proteins in the presence, but not in the absence, of Src-YF. These peptide data identified two proteins as Dok-3-associated components downstream of Src: Grb2 and Csk (Table 1). Csk was already known to be associated with tyrosine phosphorylated Dok-1, Dok-2 and Dok-3

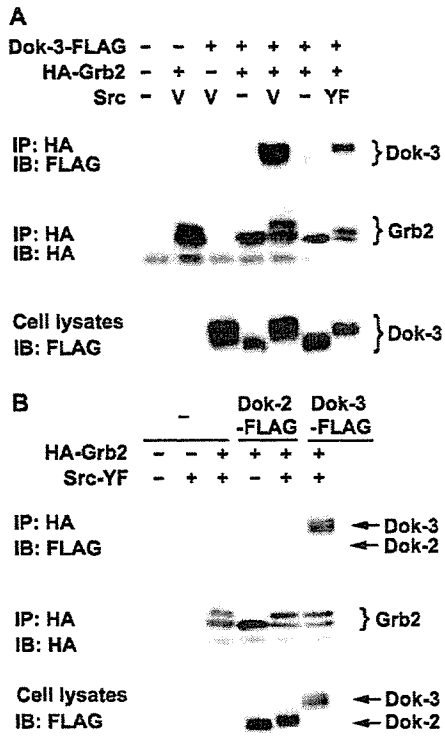

Figure 2 Grb2 preferentially binds Dok-3 downstream of Src. (A) Grb2 binds Dok-3 in a manner dependent on Src. 293T cells were transfected with expression plasmids for the indicated proteins. Anti-HA IP or whole cell lysates were subjected to IB with the indicated antibodies. V and YF stand for v-Src and Src-YF, respectively. (B) Dok-2 barely binds Grb2. 293T cells were transfected with expression plasmids for the indicated proteins. Anti-HA IP or whole cell lysates were subjected to IB with the indicated antibodies.

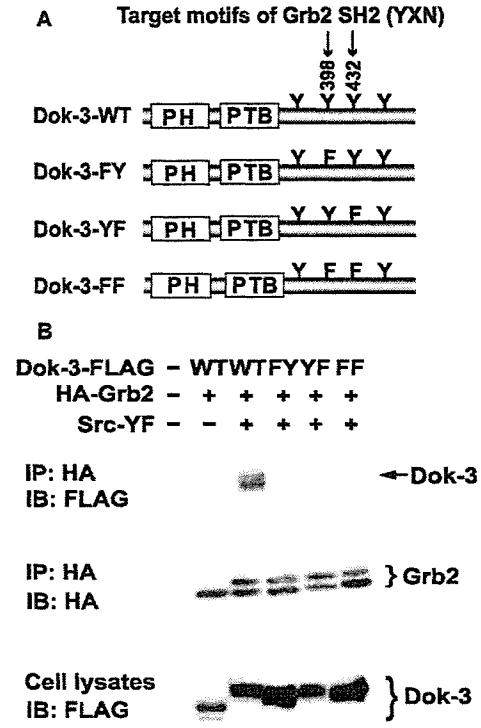

Figure 3 Tyr-398 and Tyr-432 of Dok-3 are required for Grb2 binding. (A) Schematic illustration of wild-type (WT) Dok-3 and its mutants. Positions of the PH and PTB domains and tyrosines or those substituted with phenylalanines in the C-terminal region are indicated. Tyrosines in the target motifs (YXN) of the Grb2 SH2 domain are numbered. (B) Substitution of Tyr-398 and Tyr-432 with phenylalanines abrogates the Grb2 binding activity of Dok-3. 293T cells were transfected with expression plasmids for the indicated proteins. Anti-HA IP or whole cell lysates were subjected to IB with the indicated antibodies.

(Neet & Hunter 1995; Lemay *et al.* 2000; Van Slyke *et al.* 2005). Although the biological significance of Csk binding is unclear, this at least confirmed the reliability of our assay, and therefore we further studied the interaction between Dok-3 and Grb2. Given the extremely high sensitivity of the direct nano-flow LC-MS/MS system, we first examined if Dok-3 and Grb2 form a complex in 293T cells readily detectable in immunoprecipitation and immunoblotting. As expected, forced expression of these proteins showed that Grb2 was significantly co-immunoprecipitated with Dok-3 in the presence, but not in the absence, of v-Src or Src-YF (Fig. 2A). Because both Dok-2 and Dok-3 have peptides of the form YXN, which is the optimal binding motif for the Grb2 SH2 domain (Kessels *et al.* 2002), we further examined interactions of Grb2 with Dok-2 in the presence of Src-YF and found that Dok-2 binds Grb2 to an extremely lesser extent as compared to Dok-3 (Fig. 2B).

Tyr-398 and Tyr-432 of Dok-3 are required for Grb2 binding and suppression of the Ras-Erk pathway

Because Dok-3 has two YXN motifs and its interaction with Grb2 was induced by the active form of Src, it was likely that tyrosine phosphorylation of the target motifs is essential for Dok-3 to bind Grb2 via the SH2 domain. Therefore, we generated Dok-3 mutants having Tyr/Phe substitutions at either or both of the tyrosines in the YXN motifs: (Tyr-398)-Glu-Asn and (Tyr-432)-His-Asn (Fig. 3A). The Dok-3 mutant carrying either substitution (Dok-3-FY or -YF) showed severely impaired binding to Grb2 in 293T cells in the presence of Src-YF (Fig. 3B).

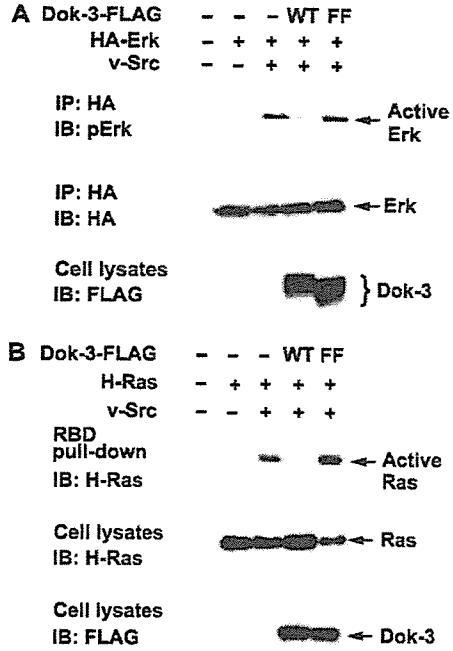

Figure 4 Grb2 binding sites are required for Dok-3 to inhibit the Ras-Erk pathway. (A) Dok-3-FF fails to suppress Erk activation. 293T cells were transfected with expression plasmids for the indicated proteins. Anti-HA IP or whole cell lysates were subjected to IB with the indicated antibodies. (B) Dok-3-FF fails to suppress Ras activation. 293T cells were transfected with expression plasmids for the indicated proteins and subsequent activation of Ras was evaluated as described in Figure 1B.

Moreover, Dok-3-FF having a substitution at these tyrosines completely lacked Grb2 binding activity. Thus, Dok-3 appears to be phosphorylated at Tyr-398 and Tyr-432 by Src so that it can bind Grb2 via the SH2 domain.

It is generally accepted that Grb2 forms a stable complex with Sos, a GEF of Ras, through the SH3 domains, and activates Ras upon recruitment via the SH2 domain by appropriate tyrosine-phosphorylated adaptors or autophosphorylated PTKs. However, it was also reported that a few adaptors bind and sequester Grb2 under certain signaling situations (Hanafusa *et al.* 2002). Therefore, we addressed the question of whether or not Grb2 binding plays a role in the inhibitory function of Dok-3 to the Ras-Erk pathway. We found that Dok-3-FF indeed has lost its ability to inhibit Erk downstream of v-Src (Fig. 4A). Consistently, this mutant did not suppress Ras downstream of v-Src (Fig. 4B), suggesting that Dok-3 sequesters Grb2 and prevents positive regulation of the Ras-Erk pathway downstream of PTKs.

Dok-3 inhibits the recruitment of Grb2-Sos complex to Shc

There is evidence demonstrating an indispensable role of Shc, an adaptor protein having the PTB and SH2 domains, in Erk activation downstream of PTKs (Lai & Pawson 2000; Ravichandran 2001; Faisal *et al.* 2004). Activation of the Ras-Erk pathway via the recruitment of Grb2-Sos complex to Shc is crucial in Src-mediated signaling (Faisal *et al.* 2004). Indeed, ectopic expression of v-Src in 293T cells induced the recruitment of Grb2 to Shc (Fig. 5A). Thus, we examined if forced expression of Dok-3 or Dok-3-FF affects the Shc-Grb2 complex formation in the presence of v-Src and found that Dok-3, but not Dok-3-FF, inhibited it (Fig. 5A). Consistently, Dok-3, but not Dok-3-FF, inhibited the recruitment of Sos to Shc (Fig. 5B). Together, our findings demonstrate that Dok-3 sequesters Grb2 and inhibits the recruitment of Grb2-Sos complex to Shc downstream of PTKs, thereby inhibiting activation of the Ras-Erk pathway.

Discussion

We recently demonstrated that mice lacking either Dok-1 or Dok-2 show a severe and lethal response to bacterial endotoxin, a lipopolysaccharide (Shinohara *et al.* 2005). In addition, mice lacking both adaptors exhibited myeloproliferative disorders, which eventually progressed into myeloproliferative disease resembling human chronic myelogenous leukemia (CML) or chronic myelomonocytic leukemia (Niki *et al.* 2004; Yasuda *et al.* 2004). These *in vivo* studies demonstrated that the Dok-family adaptors are key negative regulators of PTK-mediated signaling and help maintain homeostasis of living animals, suggesting an important role for a closely related protein, Dok-3. As mentioned earlier, Dok-1 and Dok-2 adaptors appear to recruit p120 rasGAP as an essential effector to suppress the Ras-Erk pathway (Nelms *et al.* 1998; Wick *et al.* 2001). However, as Dok-3 does not interact with rasGAP, it has been unclear how it inhibits Erk downstream of PTKs. Here, we demonstrated that forced expression of Dok-3 in 293T cells inhibits activation of Ras downstream of Src (Fig. 1), indicating a rasGAP-independent mechanism for the inactivation of Ras. Indeed, we also demonstrated that Dok-3, upon its tyrosine phosphorylation, binds Grb2 and inhibits the recruitment of Grb2-Sos complex to Shc, thereby inhibiting Ras, downstream of Src (Figs 2–5). Because two tyrosine residues, Tyr-398 and Tyr-432, of Dok-3 were essential for Grb2 binding and because each residue is in the target motif of the Grb2 SH2 domain, association of Dok-3 with Grb2 likely depends upon physical interaction between the SH2

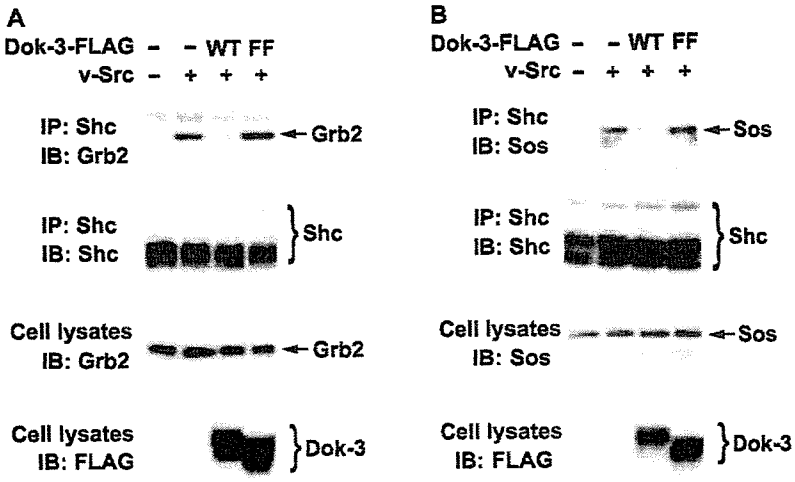

Figure 5 Dok-3 negatively regulates the recruitment of Grb2 and Sos to Shc downstream of Src. (A) Dok-3, but not Dok-3-FF, inhibits the recruitment of Grb2 to Shc. 293T cells were transfected with expression plasmids for the indicated proteins. Anti-Shc IP or whole cell lysates were subjected to IB with the indicated antibodies. (B) Dok-3, but not Dok-3-FF, inhibits the recruitment of Sos to Shc. 293T cells were transfected with expression plasmids for the indicated proteins. Anti-Shc IP or whole cell lysates were subjected to IB with the indicated antibodies.

domain and the target motifs. It is of note that Dok-2 also has an SH2 target motif; however, the binding capability of Dok-2 to Grb2 was very weak in comparison with that of Dok-3 (Fig. 2B). Thus, our findings demonstrate that Dok-3 negatively regulates Ras in a manner distinct from that of Dok-1 and Dok-2. Since these Dok-family proteins are preferentially expressed in hematopoietic cells, the Dok-3 specific pathway probably reinforces the negative regulation of Ras by Dok-1 and Dok-2 in these cells except T cell lineage where Dok-3 expression was virtually undetectable (data not shown).

Dok-1 and Dok-2 are among major phosphotyrosine-containing proteins in leukemic cells of patients with CML, which is caused by a constitutively active PTK termed Bcr-Abl (Wisniewski *et al.* 1999). We and others (Niki *et al.* 2004; Yasuda *et al.* 2004) independently reported that these adaptors work against the aberrant PTK in blastic transformation of CML-like disease in mice. Bcr-Abl has a target motif of the Grb2 SH2 domain including Tyr-177, which is an autophosphorylation site of the PTK. Thus, a Bcr-Abl mutant having a Tyr/Phe substitution at the residue loses its binding capability to Grb2. Interestingly, this amino acid substitution also impairs the transforming potential of Bcr-Abl *in vitro* and *in vivo*, demonstrating an essential role for Grb2 downstream of the PTK (Million & Van Etten 2000). Therefore, in addition to Dok-1 and Dok-2 signaling, Dok-3-mediated negative signaling may also intersect the oncogenic pathway by sequestering Grb2 from the Bcr-Abl oncoprotein, which was shown to phosphorylate Dok-3 (Cong *et al.* 1999; Lemay *et al.* 2000).

SHIP is expressed mostly in hematopoietic cells, where it acts by hydrolyzing inositol metabolites phosphorylated at the 5′ position of the inositol ring: namely, PI-(3,4,5)P3 and PI-(1,3,4,5)P4. Studies on B cell receptor-mediated signaling with *ex vivo* B cells or B cell lines lacking SHIP have provided evidence that recruitment of SHIP to FcγRIIB inhibits B cell activation by preventing PI-(3,4,5)P3 accumulation, activation of Btk and Akt, calcium fluxes, and Erk activation (Rohrschneider *et al.* 2000). Recently, Robson *et al.* (2004) reported that stimulation of B cell receptor induced tyrosine phosphorylation of Dok-3 and its binding to SHIP. They also demonstrated that forced expression of Dok-3, but not a mutant lacking the SHIP-binding site, inhibits the JNK-pathway, indicating a role for SHIP in Dok-3-mediated negative signaling. However, the recruitment of SHIP to Dok-3 did not inhibit PI-3-kinase-Akt or Ras-Erk pathway downstream of the B cell receptor. In addition, SHIP was not detected in the Dok-3-associated proteins even in the presence of Src in 293 cells (Table 1). Therefore, it is unlikely that SHIP was responsible for down-regulation of Ras in our experiments. The authors also defined a binding site of another Dok-3 partner, Csk, which inhibits Src and Src-like PTKs by phosphorylating a conserved inhibitory tyrosine residue near the C-terminus of each PTK (Robson *et al.* 2004; Roskoski 2004). Although Csk was detected in the Dok-3 associated proteins in our assay (Table 1), both Dok-3 and Dok-3-FF have an intact Csk-binding site. Moreover, Csk does not inhibit v-Src or Src-YF, because these mutants lack the inhibitory tyrosine residue by the C-terminal mutations as mentioned above. Together, at least in our assay systems, the sequestration

of Grb2 appears to be an essential event in Dok-3-mediated negative regulation of the Ras-Erk pathway. Because recruitment of Grb2 to PTKs or adaptors including Shc and FRS is critical to drive the Ras-Erk pathway in many signaling situations, further studies of Dok-3 function probably will contribute to a better understanding of the molecular bases of negative regulation in many biological events.

Experimental procedures

cDNAs and plasmids

The cDNA for human Dok-3 fused with the FLAG-tag at the C-terminus was amplified by PCR and inserted into the mammalian expression vector pcDNA3.1 (invitrogen) to generate pcDNA-Dok-3. Template Dok-3 cDNA was a kind gift from Sumio Sugano. pcDNA-Dok-3-based expression plasmids for mutants having Tyr/Phe substitutions (Dok-3-YF, FY or FF) were generated by PCR with the following primers: 5′-CAGTCCCATCTTCCACAACGGCCAGGAC-3′ and 5′-GTCAGGGTAGAAGGTGTTGCCGGTCCTG-3′ for YF; 5′-GGCAATGAGCACCTCTTTGAGAACCTGTG-3′ and 5′-CCGTTACTCGTGGAGAAACTCTTGGACAC-3′ for FY; and an appropriate combination of these primers for FF. Mouse Grb2 cDNA was generated by RT-PCR, fused with the hemagglutinin (HA)-tag at the N-terminus, and inserted into the expression vector pCAGGS (Niwa *et al.* 1991). All cDNAs were confirmed by sequencing. The expression plasmids for the following proteins were kind gifts: Erk2 fused with the HA-tag at the N-terminus from Yukiko Gotoh (Wakioka *et al.* 2001); H-Ras from Tomohiro Kurosaki (Hashimoto *et al.* 1999); and v-Src and human c-SrcY530F (Src-YF) from Tadashi Yamamoto (Kim *et al.* 2004).

Cell culture and antibodies

293 and 293T cells were maintained in Dulbecco's modified Eagle's medium supplemented with 10% fetal calf serum. The following antibodies were used for immunoblotting and/or immunoprecipitation: mouse monoclonal antibodies (mAbs) to FLAG epitope (M2) from Sigma; mouse mAbs to phosphotyrosine (4G10) and rabbit polyclonal antibodies to Shc from Upstate; rat mAbs to HA epitope (3F10) from Roche; rabbit polyclonal antibodies to phospho-Erk1/2 (pErk) from Cell Signaling; mouse mAbs to Grb2, Sos, or H-Ras from Transduction Laboratories.

Transfection

For liquid chromatography combined with collision-induced dissociation tandem mass spectrometry (LC-MS/MS), 293 cells were transfected with pcDNA-Dok-3 alone or along with pcDNA-Src-YF using Fugene 6 reagent (Roche). Cells were subjected to immunoprecipitation using M2 antibodies to FLAG epitope and an LC-MS/MS analysis at 20–24 h after transfection. Otherwise, 293T cells were transfected with the indicated plasmids by a standard calcium phosphate method, and subjected to immunoprecipitation or immunoblotting at 48 h after transfection.

Immunoprecipitation and immunoblotting

293T cells were transfected with the indicated plasmids and solubilized with TNN buffer (50 mM Tris [pH 8.0], 150 mM NaCl, 1.0% Nonidet P-40, 0.2 mM Na_3VO_4, and 20 μg/mL aprotinin). Cleared lysates were then sequentially incubated with antibodies to FLAG epitope, HA epitope, or Shc, and protein G-Sepharose (Amersham Biosciences). The immune complexes were precipitated and the immunoprecipitates were washed five times with TNN buffer. Proteins in whole cell lysates or immunoprecipitates were separated by SDS/10% or 12% polyacrylamide gel electrophoresis, transferred to PVDF membrane (Bio-Rad Laboratories), and incubated with appropriate antibodies for immunoblotting. The membranes were then incubated with horseradish peroxidase-labeled secondary antibodies (Amersham Biosciences) and the blots were visualized with an ECL system (Amersham Biosciences).

Purification and digestion of Dok-3-associated proteins

The Dok-3-associated proteins were purified and digested as previously described (Natsume *et al.* 2002; Komatsu *et al.* 2004). In brief, 293 cells transfected with pcDNA-Dok-3 alone or along with pcDNA-Src-YF were solubilized with 1 mL of TNE buffer (10 mM Tris-HCl [pH 7.5], 1% Nonidet P-40, 150 mM NaCl, 1 mM EDTA, 1 mM Na_3VO_4, 5 μg/mL aprotinin, 1 mM phenylmethylsulfonyl fluoride, 5 μg/mL leupeptin, 3 μg/mL pepstatinA, and 50 mM NaF). Cleared lysates were then incubated overnight at 4 °C with 20 μL of mAbs (M2)-conjugated agarose. The protein-bound M2-agarose beads were washed extensively with TNE buffer, and the proteins were eluted with FLAG peptide. The isolated proteins (0.2 μg of each) were precipitated using 20 μL of a methanol/chloroform mixture (1 : 1 v/v). After vacuum-drying, the precipitate was digested with 5 μL of *Achromobacter* protease I (40 pM; substrate-to-enzyme ratio 50 : 1) in Tris buffer (50 mM Tris-HCl [pH 9.0], 6 M urea, and 0.005% *n*-octyl glucopyranoside) overnight at 37 °C.

LC-MS/MS analysis

The Dok-3-associated proteins digested with *Achromobacter* protease I were analyzed using a nanoscale LC-MS/MS system as described (Natsume *et al.* 2002; Komatsu *et al.* 2004). In brief, the peptide mixture was applied to a Mightysil-PR-18 (1 μm particle, Kanto Chemical) frit-less column (45 mm × 0.150 mm internal diameter) and separated using a 0%–40% gradient of acetonitrile containing 0.1% formic acid over 30 min at a flow rate of 50 nL/min. Eluted peptides were sprayed directly into a quadropole time-of-flight hybrid mass spectrometer (Q-Tof *Ultima*, Micromass). MS and MS/MS spectra were obtained in a data-dependent mode. Up to four precursor ions above an intensity threshold of 10 counts/s were selected for MS/MS analyses from each survey scan. All MS/MS spectra were searched against protein sequences

of Swiss Prot and RefSeq (NCBI) using batch processes of the Mascot software package (Matrix Science). Criteria for match acceptance were: (1) when the match score was 10 over each threshold, identification was accepted without further consideration; (2) when the difference of score and threshold was lower than 10, or when proteins were identified based on a single matched MS/MS spectrum, the raw data were manually confirmed prior to acceptance; (3) peptides assigned by less than three y series ions and peptides with +4 charge state were all eliminated regardless of their scores.

RBD pull-down assay

A bacterially expressed glutathione S-transferase (GST) fused with the Ras-binding domain (RBD) of human c-Raf-1 (amino acids 1–149), bound with glutathione-sepharose beads was prepared as described (Taylor & Shalloway 1996). 293T cells transfected with the indicated plasmids were solubilized in a lysis buffer (50 mM Tris [pH 7.4], 100 mM NaCl, 10% glycerol, 1% Nonidet P-40, 0.5% sodium deoxycholate, 0.2 mM Na_3VO_4, and 20 μg/ml aprotinin). Cleared lysates were then incubated with GST-Raf RBD beads containing 100–200 μg of the fusion protein for 60 min at 4 °C. After extensive washing, proteins bound to the beads were boiled and eluted with SDS-loading buffer (50 mM Tris [pH 6.8], 5 mM EDTA, 100 mM dithiothreitol, 2% SDS, 0.1% bromophenol blue, and 10% glycerol) and were separated by SDS/12% polyacrylamide gel electrophoresis for immunoblotting with mAbs to H-Ras.

Acknowledgements

We thank Sumio Sugano, Yukiko Gotoh, Tomohiro Kurosaki, Junichi Miyazaki, Tohru Tezuka, and Tadashi Yamamoto for plasmids. This work was supported by Grants-in-Aid for Scientific research from the Ministry of Education, Culture, Sports, Science and Technology of Japan and by grants from the Astellas Foundation.

References

Cai, D., Dhe-Paganon, S., Melendez, P.A., Lee, J. & Shoelson, S.E. (2003) Two new substrates in insulin signaling, IRS5/DOK4 and IRS6/DOK5. *J. Biol. Chem.* **278**, 25323–25330.

Carpino, N., Wisniewski, D., Strife, A., *et al.* (1997) $p62^{dok}$: a constitutively tyrosine-phosphorylated, GAP-associated protein in chronic myelogenous leukemia progenitor cells. *Cell* **88**, 197–204.

Cong, F., Yuan, B. & Goff, S.P. (1999) Characterization of a novel member of the DOK family that binds and modulates Abl signaling. *Mol. Cell. Biol.* **19**, 8314–8325.

Crowder, R.J., Enomoto, H., Yang, M., Johnson, E.M. Jr & Milbrandt, J. (2004) Dok-6, a novel p62 Dok family member, promotes Ret-mediated neurite outgrowth. *J. Biol. Chem.* **279**, 42072–42081.

Di Cristofano, A., Carpino, N., Dunant, N., *et al.* (1998) Molecular cloning and characterization of $p56^{dok-2}$ defines a new family of RasGAP-binding proteins. *J. Biol. Chem.* **273**, 4827–4830.

Faisal, A., Kleiner, S. & Nagamine, Y. (2004) Non-redundant role of Shc in Erk activation by cytoskeletal reorganization. *J. Biol. Chem.* **279**, 3202–3211.

Grimm, J., Sachs, M., Britsch, S., *et al.* (2001) Novel p62dok family members, dok-4 and dok-5, are substrates of the c-Ret receptor tyrosine kinase and mediate neuronal differentiation. *J. Cell Biol.* **154**, 345–354.

Hanafusa, H., Torii, S., Yasunaga, T. & Nishida, E. (2002) Sprouty1 and Sprouty2 provide a control mechanism for the Ras/MAPK signalling pathway. *Nature Cell Biol.* **4**, 850–858.

Hashimoto, A., Kurosaki, M., Gotoh, N., Shibuya, M. & Kurosaki, T. (1999) Shc regulates epidermal growth factor-induced activation of the JNK signaling pathway. *J. Biol. Chem.* **274**, 20139–20143.

Hubbard, S.R. & Till, J.H. (2000) Protein tyrosine kinase structure and function. *Annu. Rev. Biochem.* **69**, 373–398.

Jones, N. & Dumont, D.J. (1999) Recruitment of Dok-R to the EGF receptor through its PTB domain is required for attenuation of Erk MAP kinase activation. *Curr. Biol.* **9**, 1057–1060.

Kessels, H.W.H.G., Ward, A.C. & Schumacher, T.N.M. (2002) Specificity and affinity motifs for Grb2 SH2-ligand interactions. *Proc. Natl. Acad. Sci. USA* **99**, 8524–8529.

Kim, M., Tezuka, T., Tanaka, K. & Yamamoto, T. (2004) Cbl-c suppresses v-Src-induced transformation through ubiquitin-dependent protein degradation. *Oncogene* **23**, 1645–1655.

Komatsu, M., Chiba, T., Tatsumi, K., *et al.* (2004) A novel protein-conjugating system for Ufm1, a ubiquitin-fold modifier. *EMBO J.* **23**, 1977–1986.

Lai, K.M.V. & Pawson, T. (2000) The ShcA phosphotyrosine docking protein sensitizes cardiovascular signaling in the mouse embryo. *Genes Dev.* **14**, 1132–1145.

Lemay, S., Davidson, D., Latour, S. & Veillette, A. (2000) Dok-3, a novel adapter molecule involved in the negative regulation of immunoreceptor signaling. *Mol. Cell. Biol.* **20**, 2743–2754.

Lowy, D.R., Zhang, K., DeClue, J.E. & Willumsen, B.M. (1991) Regulation of p21ras activity. *Trends Genet.* **7**, 346–351.

Million, R.P. & Van Etten, R.A. (2000) The Grb2 binding site is required for the induction of chronic myeloid leukemia-like disease in mice by the Bcr/Abl tyrosine kinase. *Blood* **96**, 664–670.

Natsume, T., Yamauchi, Y., Nakayama, H., *et al.* (2002) A direct nanoflow liquid chromatography-tandem mass spectrometry system for interaction proteomics. *Anal. Chem.* **74**, 4725–4733.

Neet, K. & Hunter, T. (1995) The nonreceptor protein-tyrosine kinase CSK complexes directly with the GTPase-activating protein-associated p62 protein in cells expressing v-Src or activated c-Src. *Mol. Cell. Biol.* **15**, 4908–4920.

Nelms, K., Snow, A.L., Hu-Li, J. & Paul, W.E. (1998) FRIP, a hematopoietic cell-specific rasGAP-interacting protein phosphorylated in response to cytokine stimulation. *Immunity* **9**, 13–24.

Niki, M., Di Cristofano, A., Zhao, M., *et al.* (2004) Role of Dok-1 and Dok-2 in leukemia suppression. *J. Exp. Med.* **200**, 1689–1695.

Niwa, H., Yamamura, K. & Miyazaki, J. (1991) Efficient selection for high-expression transfectants with a novel eukaryotic vector. *Gene* **108**, 193–199.

Ravichandran, K.S. (2001) Signaling via Shc family adapter proteins. *Oncogene* **20**, 6322–6330.

Robson, J.D., Davidson, D. & Veillette, A. (2004) Inhibition of the Jun N-terminal protein kinase pathway by SHIP-1, a lipid phosphatase that interacts with the adaptor molecule Dok-3. *Mol. Cell. Biol.* **24**, 2332–2343.

Rohrschneider, L.R., Fuller, J.F., Wolf, I., Liu, Y. & Lucas, D.M. (2000) Structure, function, and biology of SHIP proteins. *Genes Dev.* **14**, 505–520.

Roskoski, R. Jr (2004) Src protein-tyrosine kinase structure and regulation. *Biochem. Biophys. Res. Commun.* **324**, 1155–1164.

Shinohara, H., Inoue, A., Toyama-Sorimachi, N., *et al.* (2005) Dok-1 and Dok-2 are negative regulators of lipopolysaccharide-induced signaling. *J. Exp. Med.* **201**, 333–339.

Shinohara, H., Yasuda, T. & Yamanashi, Y. (2004) Dok-1 tyrosine residues at 336 and 340 are essential for the negative regulation of Ras-Erk signaling, but dispensable for rasGAP-binding. *Genes Cells* **9**, 601–607.

Songyang, Z., Yamanashi, Y., Liu, D. & Baltimore, D. (2001) Domain-dependent function of the rasGAP-binding protein p62Dok in cell signaling. *J. Biol. Chem.* **276**, 2459–2465.

Taylor, S.J. & Shalloway, D. (1996) Cell cycle-dependent activation of Ras. *Curr. Biol.* **16**, 1621–1627.

Van Slyke, P., Coll, M.J., Master, Z., Kim, H., Filmus, J. & Dumont, D.J. (2005) Dok-R mediates attenuation of epidermal growth factor-dependent mitogen-activated protein kinase and Akt activation through processive recruitment of c-Src and Csk. *Mol. Cell. Biol.* **25**, 3831–3841.

Veillette, A., Latour, S. & Davidson, D. (2002) Negative regulation of immunoreceptor signaling. *Annu. Rev. Immunol.* **20**, 669–707.

Wakioka, T., Sasaki, A., Kato, R., *et al.* (2001) Spred is a Sprouty-related suppressor of Ras signaling. *Nature* **412**, 647–651.

Wick, M.J., Dong, L.Q., Hu, D., Langlais, P. & Liu, F. (2001) Insulin receptor-mediated $p62^{dok}$ tyrosine phosphorylation at residues 362 and 398 plays distinct roles for binding GTPase-activating protein and Nck and is essential for inhibiting insulin-stimulated activation of Ras and Akt. *J. Biol. Chem.* **276**, 42843–42850.

Wisniewski, D., Strife, A., Swendeman, S., *et al.* (1999) A novel SH2-containing phosphatidylinositol 3,4,5-trisphosphate 5-phosphatase (SHIP2) is constitutively tyrosine phosphorylated and associated with src homologous and collagen Gene (SHC) in chronic myelogenous leukemia progenitor cells. *Blood* **93**, 2707–2720.

Yamanashi, Y. & Baltimore, D. (1997) Identification of the Abl- and rasGAP-associated 62 kDa protein as a docking protein, Dok. *Cell* **88**, 205–211.

Yamanashi, Y., Tamura, T., Kanamori, T., *et al.* (2000) Role of the rasGAP-associated docking protein $p62^{dok}$ in negative regulation of B cell receptor-mediated signaling. *Genes Dev.* **14**, 11–16.

Yasuda, T., Shirakata, M., Iwama, A., *et al.* (2004) Role of Dok-1 and Dok-2 in myeloid homeostasis and suppression of leukemia. *J. Exp. Med.* **200**, 1681–1687.

Zhao, M., Schmitz, A.A.P., Qin, Y., Di Cristofano, A., Pandolfi, P.P. & Van Aelst, L. (2001) Phosphoinositide 3-kinase-dependent membrane recruitment of $p62^{dok}$ is essential for its negative effect of mitogen-activated protein (MAP) kinase activation. *J. Exp. Med.* **194**, 265–274.

Received: 30 September 2005
Accepted: 3 November 2005

Endocrine Journal 2006, **53** (5), 567–576

REVIEW

Calpain-10 (*NIDDM1*) as a Susceptibility Gene for Common Type 2 Diabetes

YUKIO HORIKAWA

Department of Diabetes and Endocrinology, Gifu University School of Medicine, Gifu; the Laboratory of Medical Genomics, Biosignal Genome Resource Center, Institute for Molecular and Cellular Regulation, Gunma University, Gunma; Core Research for Evolutional Science and Technology (CREST), Japan Science and Technology Corporation (JST), Kawaguchi, Japan

Key words: Calpain 10, SNP, Haplotype Type 2 diabetes mellitus, *NIDDM1*

(*Endocrine Journal* **53**: 567–576, 2006)

IT is assumed that susceptibility genes associated with lifestyle-related diseases including type 2 or non-insulin-dependent diabetes mellitus (NIDDM) were positively selected for energy conservation but act adversely in modern conditions. These "thrifty genes" can be identified on the "common disease common variant" hypothesis, but detailed analysis of the genetic polymorphisms in many ethnic groups is required to clarify the molecular evolution of these susceptibility alleles. At present, single nucleotide polymorphisms (SNPs) represent the most useful data for genetic analyses of non-Mendelian polygenic lifestyle-related diseases, the common diseases including diabetes, hypertension, and obesity. Although many association studies have been conducted using single SNPs, they are problematical for several reasons, including ethnic differences within the study population, unknown environmental factors, misdiagnosed disease, and genetic mistyping. Haplotype analysis whereby several tag SNPs can be monitored simultaneously improves and complements the search. *NIDDM1* (calpain-10) is the first susceptibility gene for type 2 diabetes to be identified by this method.

Correspondence to: Yukio HORIKAWA, M.D., Ph.D., Department of Diabetes and Endocrinology, Gifu University School of Medicine, 1-1 Yanagido, Gifu-city, Gifu 501-1194, Japan

SNP and haplotype

When a single SNP is used in analysis, there are only two possible variants, but if multiple SNPs are used, there are 2^n possible variants in haplotypes, somewhat less in the case of linkage disequilibrium (LD). In addition, determination of the degree of LD by LD coefficients (*e.g.*, D, d^2, r^2) permits estimation of the physical map distance from a susceptibility gene, narrowing a disease locus to 10–100 kb. Thus, LD mapping of haplotypes is potentially more fruitful in screening susceptibility genes for common diseases. When marker SNPs and a putative disease susceptibility allele are located in the same LD block, haplotype structure analysis is relevant for any variant regardless of its frequency. On the other hand, if the putative disease allele is not located in an LD block with the SNP markers, single SNP analysis may yet be more useful than analysis of the haplotype structure [1].

A meta-analysis assessed the collected data on single SNPs in a comprehensive manner to screen candidate polymorphisms for polygenic diseases, and found only 16% of the candidate polymorphisms to have a significant genetic association that could be replicated without heterogeneity or bias. However, the majority of these candidate polymorphisms were false-positive results, attributed later to insufficient sample size or first versus subsequent discrepancies [2]. LD analyses using single SNPs are clearly liable to type I errors, while simultaneous assay of several SNPs contained in haplotype reduces the confounding effects of ethnic